치의과학 박사학위논문

Transcriptional signature profiling of terminal differentiation and replicative senescence in human oral keratinocytes

사람 구강각화세포의 최종분화 및 복제노화 과정에서
유전자 발현 프로파일링

2017 년 8 월

서울대학교 대학원
치의과학과 종양 및 발달 생물학 전공
장 다 현

Transcriptional signature profiling of terminal differentiation and replicative senescence in human oral keratinocytes

지도교수 민 병 무

이 논문을 치의과학 박사학위논문으로 제출함

2017년 4월

서울대학교 대학원

치의과학과 종양 및 발달 생물학 전공

장 다 현

장다현의 박사학위논문을 인준함

2017년 6월

위 원 장 _____ (인)

부위원장 _____ (인)

위 원 _____ (인)

위 원 _____ (인)

위 원 _____ (인)

ABSTRACT

Transcriptional signature profiling of terminal differentiation and replicative senescence in human oral keratinocytes

Dahyun Jang

Department of Cancer and Developmental Biology

Graduate School

Seoul National University

(Directed by Prof. Byung-Moo Min, D.D.S., M.S., Ph.D.)

Somatic cells have limited replication capacity, and after a finite number of cell divisions, DNA damage is triggered by telomere shortening; thus, the cells enter a state called replicative senescence, where DNA is unable to replicate and cell replication is irreversibly stopped. In addition, the cells that undergo replicative senescence show great differences in morphology and gene expression, even though they maintain their metabolic activity. Although there are many studies on the genes associated with differentiation and senescence, there is little information on the analysis of related genes and their gene network involved in the terminal differentiation and

replicative senescence. Therefore, this study aimed to examine comprehensively the changes in the expression of the genes involved in the final differentiation and senescence process and their gene networks and functions. Isolated normal human oral keratinocytes (NHOKs) were subcultured continuously to obtain the terminally differentiated and replicative senescent cells; the state of terminal differentiation or replicative senescence of the cells was verified at the protein and RNA level. The total RNAs were isolated from rapidly growing NHOKs and replicative senescent NHOKs were analyzed by microarrays using Affymetrix Human Genome U133 Plus 2.0 Array, the results were confirmed by real-time RT-PCR, and the gene set with altered expression were run though the bioinformatical analysis software Ingenuity Pathway Analysis (IPA). Microarray results showed increased expression in 1,247 genes and reduced expression in 1,219 genes. The greatest number of these altered genes was identified as being related to biological pathways of transport, cell proliferation, cell cycle, defense and immune response, cell death, transcription, apoptosis, and inflammatory response. Several highly-upregulated genes of inflammatory response (IL-1β, S100A8, S100A9, MMP1, MMP9, IL-8, BHLHB2, HES1, and TWIST1) were observed following the serial subculture in NHOKs. As the terminal differentiation and replicative senescence of NHOKs occurred, the expression of inflammation-related genes such as IL-1β and IL-8 increased. Next, in order to investigate these inflammatory genes involved in NHOKs terminal differentiation and replicative senescence, IL-1β was treated to rapidly proliferating NHOK cells for 12 to 96 hours, and terminal differentiated and replicative senescent cells were treated with IL-1β neutralizing antibody for 14 days. There was an increased IL-1β, S100A8, S100A9, MMP1, MMP9 and IL-8 expression of rapidly dividing NHOKs when treated with IL-1β, and there was a decreased gene expression of senescing NHOKs when treated with IL-1β neutralizing antibodies. Furthermore, in order to confirm this *in vivo*, the expressions

of the genes related to the differentiation or senescence were confirmed by immunocytochemistry in gingival tissues of 3-month old and 2-year old mice. Involucrin, $p16^{INK4A}$, DEC1 (Bhlhb2) and IL-1β were strongly expressed in gingival tissues of 2-year-old mice compared to that of 3-month-old mice. Overall the experiments described in this thesis presents a comprehensive analysis of the gene expression pattern of the terminal differentiation and replicative senescence process of NHOKs; these results show altered expression of genes associated with biological function of protein transport, cell proliferation, cell cycle, defense and immune response, cell death, transcription, apoptosis, and inflammatory response. The purpose of this study was to lay the groundwork for the understanding of the terminal differentiation and senescence process of NHOKs by investigating the genes related to senescence through the functional analysis of gene expression changes.

Keywords: Human oral keratinocytes, cell differentiation, replicative senescence, gene network

***Student Number*:** 2008-22047

CONTENTS

LIST OF TABLES

LIST OF FIGURES

BACKGROUND

Keratinocytes

The keratinocyte is the principal cell type in the epidermis, primary function of keratinocytes is to provide the structural and physical integrity of the skin, thereby protecting the body against external injury. Epidermal keratinocytes residing in the basal layer of the epidermis differentiate through multiple layers and finally shed as cornified dead cells from the skin surface (1,2). The epidermis is composed of four layers, the stratum basal layer, spinous layer, granular layer and the stratum corneum. The basal layer in normal adult epidermis is restricted proliferative capacity. The products of this proliferative process eventually become the post-mitotic cells of the basal layer that are committed to the differentiation program. Thus, the epidermis is maintained in a state of self-renewal, with continuous proliferation in the basal layer replacing the keratinocytes that are shed from the outermost cornified layer (3). The next layer is the spinous layer which consists of multiple layers of keratinocytes becoming progressively more flattened with increasing distance from the basal layer. In the spinous layer, the synthesis of new keratins begins and these proteins are assembled into dense bundles giving the cells a characteristic appearance when visualised by transmission electron microscopy (4). As keratinocytes enter the granular layer, major differentiation events become evident and markers of differentiation are expressed. The first differentiation event is keratinization. The second major differentiation-associated event is keratohyalin deposition. The most prominent

morphologic feature of keratinocytes of the granular layer is protein-rich granules called keratohyalin granules (5). These granules contain profilaggrin, which is a precursor molecule to filaggrin. Filaggrin or filament-aggregating protein, facilitates the alignment and aggregation of keratin filaments into tightly packed bundles in the cornified cell. Filaggrin hydrolysis is a tightly regulated process by which profilaggrin is dephosphorylated and proteolytically cleaved first into oligomeric, dimeric, and then monomeric subunits and ultimately into amino acids in the outer layers of the stratum corneum (6). Free amino acids contribute to the water-holding properties of the stratum corneum. The third differentiation event is formation of the cornified envelope, sometimes referred to as cell cornification. The proteins involucrin, keratolinin, loricrin, and pancornulins are precursor proteins synthesized in the granular layer. They ultimately become cross-linked by the enzyme transglutaminase. This results in formation of a rigid structural ectoskeleton that serves as a scaffolding for insertion of keratin filaments and a barrier to the external milieu. The stratum corneum is the outermost layer of the skin and is composed of corneocytes, which are basically anucleate, nonviable keratinocytes that are organized into geometric stacks embedded in a lipid-rich intercellular matrix. It is the stratum corneum that provides the skin's important barrier functions, such as protecting the body against water loss and against entrance of infection, physical and/or chemical injury (7).

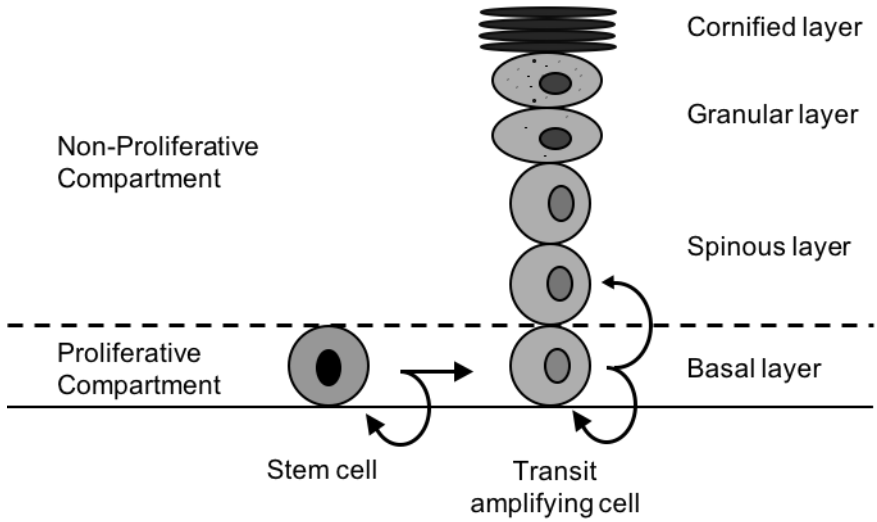

Figure 1. Schematic representation of keratinocyte differentiation.

Isolation of Keratinocytes

In vitro cell culture is a necessary prerequisite in acquiring a thorough understanding of the biology and behavior of the cells of interest and is a critical first step in developing cellular therapies. An ability to grow and manipulate primary epithelial keratinocytes *in vitro* is essential to gain insights into the biology of skin that may have clinical implications. The dissociation methods of keratinocyte primary culture are well established. There are basically two techniques in primary culture: the direct explant and the enzymatic technique. Carrel and Burrows described in 1910 a method for the extraction of epithelia cells called direct explant (8). The direct explant technique has been used in the culturing of human gingival (9). The explant technique has two advantages: The direct explant technique obtained the first keratinocytes yield faster than the enzymatic technique, and technical handling involved in the direct explant method at the beginning of the process has fewer steps (10).

The enzymatic technique was developed by Daniels et al. (1996), who surveyed the success rate of human keratinocyte isolation with various concentrations including trypsin and dispase (11). For the isolation of the cells it is necessary to dissociate the dermal and epidermal layer without destroying the cells, which is carried out nowadays with enzymes, dispase and collagenases, to release the fibroblasts from the dermis (12). Collagenases and dispase are formulated for efficient dissociation of tissue from a wide variety of sources. Cells were isolated from human foreskin or gingiva tissue to the one-step enzyme incubation procedure using collagenases II and dispase.

Differentiation of Keratinocytes

Epidermal differentiation begins with the migration of keratinocytes from the basal layer, and ends with the formation of the cornified layer. The rapidly dividing basal keratinocytes are devoted to amplifying the epidermal cell population and produce a sufficient number of daughter cells that migrate out of the basal layer towards the suprabasal layer at the onset of terminal differentiation (13). Cells in the upper layers of the cells lose their ability to divide, then exhibit morphological changes that result from the progressive maturation of cell structures associated with their upwards migration. In spinous and granular layers, keratinocytes continue to prepare the keratinization process. The keratinocytes in the stratum corneum are dead squamous cells that are no longer multiplying. When the keratinocytes reach the corneum, they are said to be keratinized creating the tough outer layer of skin (14).

Keratinocyte differentiation is associated with changes in gene expression, specifically of keratin genes, keratins being the most abundant epidermal proteins. Keratinocytes of the basal epidermal layer express keratins K5 and K14. Upon differentiation, when keratinocytes exit from the basal layer and migrate upwards into the suprabasal layers, these keratins are substituted by K1 and K10 (15,16,17). The K5/K14 pair is expressed in the basal layer of the epidermis, which contains epidermal stem cells and transient amplifying (TA) cells, while the K1/K10 pair is synthesized only in post-mitotic keratinocytes. Basal keratinocytes migrate from the basal into the spinous layers, lose their mitotic activity, and begin to synthesize a new set of structural proteins and enzymes that are characteristic of cornification. The K1/K10 are among the first proteins to be expressed during cornification

(18). In the granular layers, filaggrin and precursors of the cornified envelopes such, as loricrin and involucrin, as well as epidermal transglutaminase are expressed (19,20,21,22). These are the cornified-envelope proteins, a complex series of lipids are synthesized, some of which become covalently attached to proteins of the cornified envelope, and most of which form intercellular lamellae that help produce a complete barrier. So, the cornified layer is composed of terminally differentiated, dead, cornified, flattened cells that are known as corneocytes. These corneocytes mostly consist of keratin intermediate filaments embedded in a filaggrin matrix and surrounded by insoluble lipids. Corneocytes are tightly attached to each other by modified desmosomal structures, which are proteolytically degraded in the uppermost layers of the cornified layer to allow desquamation (23).

Keratinocyte differentiation *in vivo* can be modulated by the local environment, for example directly by mesenchymal epithelial interactions or indirectly by cytokines produced by other cell types. Despite this dependence on environmental influences, it is known that the tendency of keratinocytes to stratify and differentiate is retained *in vitro*, even in the absence of instructive information from the connective tissue stroma and/or other cells (24). Basal cells of different epithelia which have diverged irreversibly from each other during development and use different program of differentiation, maintain this information even after serial passaging (25,26). These findings suggest that a culture system for human epidermal keratinocytes can be a good model for cellular growth and differentiation, especially to study the effect of the local environment.

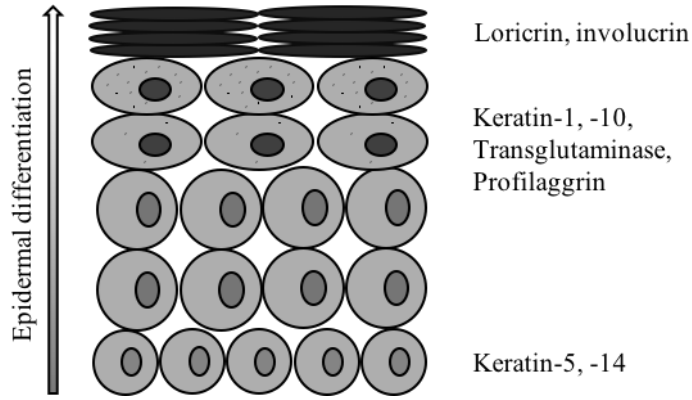

Figure 2. Terminal differentiation in the epidermis. The proteins that are expressed in particular locations in the epidermis during differentiation are shown.

Cellular Senescence

Cellular senescence has been defined as the terminal phase of passaged primary cell populations (27). It is in fact a biologically irreversible state of cell growth arrest for which some investigators prefer the more precise term of replicative senescence (28). The senescence growth arrest is essentially permanent and cannot be reversed by known physiological stimuli (27). Cellular senescence refers to an irreversible fate of damaged cells that is induced by a variety of stressors, including end of replicative lifespan, oncogenic stimuli, DNA damage, and mechanical stress (27,28,29,30). Unlike apoptosis, which results in the elimination of damaged cells, senescence leads to viable and metabolically active cells which have permanently arrested replication through a complex and multi-faceted cellular programming (31,32). A prime cause of replicative senescence in human cells is progressive telomere shortening (33,34,35). Telomeres consist of repetitive DNA elements at the end of linear chromosomes that protect the DNA ends from degradation and recombination (36,37). Due to the intrinsic inability of the replication machinery to copy the ends of linear molecules, telomeres become progressively shorter with every round of cell division (38). Finally, telomeres reach a short length, behaving as double-stranded DNA breaks in telomere initiated senescence or apoptosis (39). Without telomeres dysfunction, DNA damage involve the induction of replicative senescence by telomere attrition has been established (40,41). DNA damage accumulates with age and that this may be due to an increase in production of reactive oxygen species (ROS) and a decline in DNA repair capacity with age (42,43).

Senescent cells have several different characteristic functional and morphologic phenotypes. (a) Most senescent cells also express the tumor suppressor protein $p16^{INK4A}$ (44,45,46). This protein activates the retinoblastoma (RB) gene whose primary function is to repress transcription genes needed for cell cycle (47). Tumor suppressor protein $p16^{INK4A}$ is believed to be a late marker of a sustained DNA damage response and its expression is found to be increased with age. (b) Senescent cells also express a senescence-associated β-galactosidase (SA-β-gal), which is reflected by the increase in lysosomal mass, but, there is no clear evidence pointing to an actual involvement of this enzyme in the senescence response (27). Commercially available products are available that allow identification of SA-β-gal in cytoplasm of senescent cells, resulting in blue staining cells. SA-β-gal is the most widely used marker of senescence; however there is no universal or specific marker for cellular senescence (48). (c) Senescent cells obtain distinct phenotypic traits, including chromatin modifications and profound changes in protein secretion, which are referred to as the senescence-associated secretory phenotype (SASP) (49). Senescent cells increase in size, sometimes enlarging more than twofold relative to the size of nonsenescent counterparts (50).

Microarray

Microarray allow many genes to be studied in the same experiment rather than one gene at a time. It provides huge amounts of data quickly and it will help understand the complex

relationships between individual genes. Microarray has been used to elucidate wide gene expression profiling, protein binding site and single nucleotide polymorphism (SNP) (51).

Changes in gene expression are associated with numerous biological processes, cellular responses and disease states. The availability of microarrays has made it possible to study gene expression in a high-throughput fashion and gather insights about biology and disease. In recent years, a massive amount of microarray studies has been conducted and numerous datasets generated. Microarray platforms enable the comparison of thousands of genes expressed in a cell at any given time which are simultaneously monitored; they have been applied to study the effects of development and ageing on gene expression (52).

The gene expression profile can be observed with spotted microarray of short segments of DNA oligonucleotides representing whole genome of an organism which is then hybridized with fluorescent labeled cDNA probes synthesized in bulk from mRNA. The fluorescent intensity of a spot reflects the relative expression level of each corresponding gene. The labeled cDNA probes have been prepared by direct incorporation of Cy3 or Cy5 labeled dNTP. Alternatively, chemically modified dNTP can be used to improve fluorescence intensity (https://www.affymetrix.com).

Microarray analysis attempt to extract biological meaning from massive amounts of gene expression data. Clustering has been one of the most successful methods for extracting coordinately regulated sets of genes. A system of cluster analysis for genome-wide expression data from microarray hybridization is described that uses standard statistical algorithms to arrange genes according to similarity in pattern of gene expression. The output is displayed graphically, conveying the clustering and the underlying expression data simultaneously in a form intuitive for biologists. Gene expression clusters can be

assigned to the gene ontology terms or pathway resources using annotations from public databases (53). Gene Ontology (GO) provides a powerful source of information to be used to cluster annotation based on biological background. The GO is a resource, in the form of a structured ontology, which describes and categorizes gene product functions in distinct categories and the relationships between them. The GO functional categories are classified in three general categories: biological process, molecular function, and cellular component. The biological process category contains individual GO terms that describe processes associated with molecular events and pathways representing multiprotein-dependent functions. The molecular function category, in contrast, describes basic gene functions at the molecular level. Lastly, the cellular component category describes the location, environment, or part of the cell, so that the gene product can be located (54,55).

INTRODUCTION

Normal human somatic cells undergo a limited number of cell proliferation, eventually reaching an irreversible cell cycle arrest known as replicative cellular senescence (12,56). Senescent cells remain viable and metabolically active, but are unable to proliferate despite the presence of mitogens and nutrients (27). The number of times that a cell divides before entry into senescence is highly variable, depending on the cell type and the organism from which it was originally derived.

In a previous study, the senescence is a complex process that regarding to the cellular senescence and decreased proliferative ability, reduction of cellular DNA repair capacity, loss of telomeres with advancing age (30,56), point mutations of extranuclear mitochondrial DNA (mtDNA) (28), increased oxidative stress and increased frequency of chromosomal abnormalities (12,57,58,59). Human aging is developed from such an accumulation of the molecular mechanisms. Despite these advances our knowledge on human ageing still remains limited.

Among the normal human somatic cells, epidermal and mucosal keratinocytes migrate from the basal layer to the surface (60), where they terminally differentiate, arrest cell cycle at G1, and ultimately lose their nuclei to become corneocytes *in vivo* (59). Terminal differentiation of keratinocytes shows proliferation arrest, which is known as replicative senescence. Replicative senescence results from prolonged proliferation in culture of primary cells after serial passaging *in vitro* (29). Primary NHOKs underwent approximately 19~25 population doublings (PD) when serially subcultured (61). Furthermore, senescent keratinocytes exhibit SA-β-gal activity (27). $p16^{INK4A}$ protein has

also been associated with cellular senescence in oral keratinocytes (44,61). Although previous studies have demonstrated that adult oral keratinocytes undergo differentiation and senescence (44,62), however, the knowledge about the regulatory network that receives senescence signals and initiates the senescence response is still lacking.

To better understand the network of genes involved in the senescence process in NHOK, we performed microarray based gene expression profiling in exponentially replicating cells compared with senescent cells. Microarrays are used to measure the transcript abundance, or levels of gene expression of mRNA transcribed from each gene in the genome (53). A vast amount of gene lists can be uploaded into the server and used to identify molecular networks, key biological functions and common cellular pathways by using a bioinformatics software such as IPA. This technology has provided an opportunity into the genome-wide expression patterns, like cellular signaling, cellular growth, cellular development and functions of terminal differentiation and replicative senescent cells (63). Identifying differentiation and senescence regulated functional gene groups based on regulatory and gene expression information. Above all, *in vitro* and *in vivo* studies exhibited a close relationship between differentiation and senescence of NHOKs. A major goal in keratinocyte biology is to identify genes, pathways, and networks that control differentiation and senescence.

MATERIALS AND METHODS

Culture of Primary Cell

Primary normal human oral keratinocytes (NHOKs) were prepared from keratinized oral epithelial tissues according to methods previously reported (64). Briefly, Healthy human gingival tissue specimens obtained from patients (age range 20 to 50 years) who were undergoing oral surgery. The gingival tissue samples were washed three times with Hanks' balanced salt solution (HBSS; GIBCO) supplemented with 0.03% sodium bicarbonate (GIBCO). To separate epithelial layer from underlying fibrous connective tissue, the tissues were incubated in HBSS containing collagenase (type II, 1.0 mg/ml; Sigma-Aldrich) and dispase (grade II, 2.4 mg/ml; Boehringer-Mannheim) for 90 minute at 37°C in humidified 95% air and 5% CO_2. Primary oral keratinocytes were prepared from separated epithelial tissue by trypsinization and maintained in complete keratinocyte growth medium (KGM; Lonza) supplemented with bovine pituitary extract, recombinant human EGF, insulin, hydrocortisone, gentamicin. Approximately 70% confluent primary NHOK were plated at $1x10^5$ cells per 60-mm culture dish, cultured for 7-10 days. The confluent primary cells were dissociated using 0.125% trypsin-EDTA (GIBCO) and then used for subculture.

Generation of Cell Differentiation and Replicative Senescence

NHOKs were serially subculture was performed when the cells reached 70% confluence. NHOKs were plated at $1x10^6$ cells per 100-mm culture dish and cultured until the cells reached 70% confluence. Every 70% confluence until they reached the post-mitotic stage of proliferation, at which time the culture was maintained for 12 days without further passage.

Cell Culture and Treatment

NHOKs were cultured under standard conditions (humidified atmosphere, 5% CO_2 at 37°C) in keratinocyte growth medium (KGM; Lonza) supplemented with bovine pituitary extract, recombinant human EGF, insulin, hydrocortisone, gentamicin; media were replaced every 48 hours. To determine the cellular senescence by IL-1β induction, proliferating NHOKs were incubated with 10 ng/ml of recombinant human IL-1β for 12, 24, 48, 72, and 96 hours, or 0.1% BSA. To identify the protection of cellular transformation by IL-1β, senescing NHOKs were treated for 14 days with 10 ng/ml of human IL-1β/IL-1F2 neutralizing antibody. The exponentially growing NHOKs reached 70% confluent, required sub-cultured to survive.

Determination of Population Doublings

Isolated NHOKs were plated in 60-mm culture dishes. Three days after seeding, the number of cells that had been originally plated was determined by colony counting. Cells were cultured until they reached 70% confluence and then the cell numbers in the dishes were counted in a hemocytometer. This count allowed determination of the number of PD of the primary cultures. And the cumulative PD were determined based on the number of NHOK harvested at every passage. The PD was calculated at the end of each passage by the formula, 2^N = (Cf/Ci), where *N* denotes the number of PDs; Cf, the total number of cells harvested at the end of a passage; and Ci, the total cell number of attached cells at seeding.

SA-β-gal Staining

Senescent NHOKs were identified by their ability to stain positively for β-galactosidase, as previously described (27). Briefly, cells were fixed with 3% formaldehyde/ 0.2% glutaraldehyde for 10-15 minute at room temperature. The cells were then stained for SA-β-gal activity in freshly prepared staining solution. Staining was evident for 12-16 hours at 37°C (no CO_2). The presence of β-galactosidase activity was evidenced by a blue color in the perinuclear cytoplasmic region.

Western Blot Analysis

Western blot analysis was performed as in previous report (64). Briefly, whole cell extracts from the cultured cells were isolated using lysis buffer (50 mM Tris-HCl [pH = 7.4], 150 mM NaCl, 1 mM EDTA [pH = 8.5], 1% Triton X-100, 1% sodium deoxycholate, 0.1% SDS, 1 mM β-glycerophosphate disodium salt hydrate, 2 mM sodium orthovanadate, and 1 mM phenylmethanesulfonyl fluoride [PMSF]; Sigma-Aldrich) and then separated by SDS-polyacrylamide gel electrophoresis (PAGE) and transferred to Immobilon protein membranes (Millipore). The membranes were incubated with the primary antibodies and probed with the respective secondary antibodies conjugated with HRP. Antibodies for involucrin (SY5; Sigma-Aldrich), transglutaminase (Ab-1; Oncogene), $p16^{INK4A}$ (C-20; Santa Cruz), and β-actin (20-33; Sigma-Aldrich). Antigen-antibody complexes were visualized using ECL Western blotting detection system (Intron biotechnology).

Reverse Transcription-Polymerase Chain Reaction (RT-PCR)

Purification of total RNA was prepared from the cultured NHOKs at 8 different time points (PD 10.0, 12.1, 14.1, 17.0, 19.4, 21.3 and 21.6) of keratinocyte differentiation and senescence using the RNeasy Mini kit (Qiagen). Total RNA was reverse transcribed to cDNA, which was used for PCR amplification of involucrin (31 cycles), transglutaminase (27 cycles), $p16^{INK4A}$ (36 cycles), and GAPDH (27 cycles, denaturation at 95°C for 20

second, annealing at 60°C for 10 second, and extension at 70°C for 10 second). The RT-PCR primers used for analysis of involucrin, transglutaminase, $p16^{INK4A}$, and GAPDH genes were represented in Table 2. The PCR products were electrophoresed on a 1.5% agarose gel, followed by ethidium bromide staining, and visualized using a UV illuminator.

Real-Time RT-PCR

Total RNA was isolated from the cultured cells using TRI-reagent (Molecular Research Center) and purified through RNeasy Mini kit (Qiagen). The cDNA was prepared using SuperScript™ III Reverse Transcriptase (Invitrogen) and a random hexamer and then subjected to real-time PCR amplification using SYBR® Green PCR Master Mix (TaKaRa). The quantitative real-time RT-PCR analyses were performed using a 7500 Real-time PCR System (Applied Biosystems). The thermal cycling for all reactions was follows: 95°C for 4 minute, followed by 40 cycles of 95°C for 15 second, 60°C for 20 second and 72°C for 34 second. Real-time RT-PCR primers used for analysis of involucrin, transglutaminase, $p16^{INK4A}$, and GAPDH genes were represented in Table 2. Each assay was normalized to GAPDH or HPRT1 mRNA levels. In addition, the real-time RT-PCR primers used for analysis of network genes were represented in Tables 3-7. The real-time RT-PCR primers used for analysis of inflammatory genes after IL-1β treatment were represented in Table 8.

Flow Cytometry

Cells plated at a density of $4x10^6$ cells/100-mm culture dishes were cultured and detached by gentle treatment 0.125% trypsin-EDTA (GIBCO) in DPBS. Cells were collected, washed once with cold DPBS and fixed in 70% ice-cold ethanol at 4°C for 30 minute. Cells were washed twice with DPBS and incubated for 30 minute at 37°C in 0.5 ml DPBS containing 100 μg/ml RNase A, 50 μg/ml propidium iodide (Sigma-Aldrich), and 0.05% Triton X-100. The cell cycle phases (Sub-G1/G0, G1, S, G2/M) of each group were calculated using the cell DNA content reflected by PI fluorescence intensity. The data were obtained using the flow cytometer FACSCalibur (BD Biosciences).

Microarray Analysis

Gene expression profiling was performed between exponentially growing keratinocytes (PD 14.1) and terminally differentiated and senescent keratinocytes (PD 21.6), using the GeneChip™ Human Genome U133 Plus 2.0 Array from Affymetrix. Total cellular RNA was isolated from the cultured NHOKs (PD 14.1 and PD 21.6) using TRI-reagent (Molecular Research Center) and further purified through the RNeasy Mini kit (Qiagen). cDNA was synthesized using a GeneAmp RNA PCR kit (Applied Biosystems) from the extracted total RNA samples. Labeled cRNA was synthesized using a Quick Amp labeling kit (Agilent Technologies) according to the standard protocol. For hybridization, cy3-

labeled cRNA from RNA samples of proliferating keratinocytes (PD 14.1) or terminally differentiated and senescent cells (PD 21.6) was hybridized to a GeneChip™ Human Genome U133 Plus 2.0 Array (Affymetrix) according to the manufacturer's protocol. The expression profiling of more than 47,000 annotated genes was compared rapidly proliferating cells (PD 14.1) and replicative senescent cells (PD 21.6). Arrays were scanned using Agilent microarray scanner (Agilent Technologies), and the scanned images were captured using Agilent feature extraction software. The data was imported into GeneSpring GX software (Agilent Technologies) for the selection of up-regulated and down-regulated genes. By applying more stringent criteria and including only genes that showed a significant ($P < 0.05$) expression difference of at least 2-fold between PD 14.1 and PD 21.6 cells. Expression levels in the samples were normalized to the media of the corresponding sample. Genes with an expression up- or down-regulated by at least two-fold were used for further analysis with IPA. The results obtained from the microarray analysis were confirmed by real-time reverse transcription-polymerase reaction (RT-PCR) of selected genes in the senescence associated genes.

Ingenuity Pathways Analysis

Comparative analysis of gene microarray data was performed using an IPA software version 4.0 (Ingenuity Systems) (51). IPA identified significant gene networks, top functions and canonical pathways associated with the differentially expressed genes for

each comparison analyzed. A detailed description of IPA can be found on http://www.quagen.com/Ingenuity.

Immunohistochemistry

In situ expression of involucrin, $p16^{INK4A}$, IL-1β, DEC1 and VEGF were determined in tissue specimens by immunohistochemistry. Mouse gingival tissues were obtained 3-month-old mice and 2-year-old mice. Mouse gingival tissues dissected and fixed immediately by formalin. Tissue specimens were processed for paraffin wax embedding and 4μm sections were prepared from each block for examination. Involucrin (1:200; Abcam), CDKN2A/p16INK4a (1:200; Abcam), IL-1β (1:200; Santa Cruz), DEC1 (1:100; gift from Y Kato, Hiroshima University Graduate School of Biomedical Sciences, Hiroshima, Japan), and VEGF (1:100: Santa Cruz) antibodies were used as primary antibodies. CSA system (DAKO) was employed. Sections were initially immersed in Target Retrieval Solution (DAKO) at 97°C for 20 minute, and subsequent steps were performed according to the manufacturer's instructions. The immunostaining of all mice gingival tissue specimens was performed simultaneously to ensure the same antibody reaction and DAB exposure conditions.

Statistical Analysis

For real-time RT-PCR experiments were performed at least triplicate. The data were expressed as the mean ± standard deviation (SD). Comparisons between multiple groups was analyzed using a one-way analysis of variance (ANOVA) followed by Student's *t*-test. A statistically significant difference was indicated when the *P*-values less than 0.05.

RESULTS

Serial Subcultures of Primary NHOKs

Primary NHOKs cultures from three different donors were prepared from separated epithelial tissue. Three days after seeding, colonies of rapidly dividing NHOK and serially subcultures until they have irreversibly lost the ability to proliferate. NHOKs reached the senescent phase of proliferation, at that time the culture was maintained for 12-14 days without further passage. NHOKs were serially subcultures until the cells stopped division, and the numbers of cumulative population doublings were determined at each passage. Normal human cells PD only a finite number of times, depending on cell type, donor age and genotype, and history of the tissue. Changes in the morphological features of NHOKs during *in vitro* culture were examined by phase contrast microscopy at different PD of replication. Lower PD (<PD 14.1) of primary NHOKs displayed the typical keratinocyte morphology and retained an undifferentiated phenotype. NHOKs showed signs of differentiation when they reached PD 19.4 (Fig. 3a) but, the majority of the cells at this doubling level still maintained the replicating epithelial cell morphology. At PD 21.6, non-dividing cells displayed the characteristics of terminal differentiation, including a flat, highly enlarged and elongated cytoplasm, and terminally differentiated cells started to round up and detach from the culture dish (Fig. 3a). On the basis of the shape of the proliferation curve (Fig. 3b), NHOKs proliferated well until passage number 4, constituting the log phase of the growth curve. NHOKs past passage number 5 exited from the log phase

of cell proliferation and apparently proliferated at a markedly reduced rate. After passage number 7 or 8, there were not enough cells to establish the subsequent passage, and the serial subculture was stopped at this point. To understand the distinction between replication, differentiation, and senescence of NHOK *in vitro*, we determined the morphological features, molecular markers of keratinocyte differentiation and senescence, and staining of cells for SA-β-gal activity.

Serial Subcultures Induce Cell Differentiation of NHOKs

Differential expression of involucrin and transglutaminase which is the molecular markers for keratinocyte differentiation (12,58,61). To detect keratinocyte differentiation, Western blot, real-time RT-PCR, and RT-PCR, were employed to examine the NHOKs cultures at different time points (Fig. 4a-c). During the proliferative phase, faint or weak expression was observed for involucrin and transglutaminase proteins (Fig. 4a). The expression of involucrin and transglutaminase gradually increased to a maximum after the beginning of the senescent phase after the majority of the cells had stopped dividing (Fig. 4a-c). These results indicate that serial subculture of primary NHOKs induces keratinocyte differentiation.

Serial Subcultures Induce Replicative Senescence of NHOKs

Cell senescence was assessed by $p16^{INK4A}$ expression and β-galactosidase staining analysis. $p16^{INK4A}$ protein is reported in studies on the replicative senescence of normal human epidermal keratinocytes (65), and is believed to be an essential element in senescence. $p16^{INK4A}$ levels are low or undetectable in exponentially growing phase, but significantly increased in the serially subcultured keratinocytes with increasing PD numbers (Fig. 5a-c). In particular, the level was extremely high in cultures at the senescent stage (PD 21.6).

Morphological features of NHOKs during serial cultures were examined by phase contrast microscopy at different PDs (PD 12.1 and PD 18.1). Exponentially growing cells (PD 12.1) were undifferentiated phenotype, small and polygonal in shape with large nuclei containing prominent nucleoli (Fig. 5d, left). Non-dividing cells at PD 18.1, most cells displayed the characteristics of replicative senescence, such as larger overall, and contained clear round and vacuolated spaces in the perinuclear cytoplasm (Fig. 5d, right). Cells in the senescing phase (PD 18.1) were larger with a proportionately larger cytoplasmic compartment. The most notable change in cells entering senescence was a dramatic increase in the number and size of clear vacuoles that occupied most of the perinuclear cytoplasm.

Senescence associated-β-galactosidase activity is a useful marker for senescent cells. Increased SA-β-gal activity, G1 cell cycle arrest and decreased telomerase activity are classic characteristics of senescent cells (27). In order to determine if the replicative senescence results from the serial subcultures of NHOKs, the SA-β-gal activity was determined. The percentage of 70-80% cells at PD 18.1 displayed characteristics of

replicative senescence, showing SA-β-gal positive staining (Fig. 5e, right). The combined results from use of both $p16^{INK4A}$ and SA-β-gal indicate that serial subculture of primary NHOKs induces replicative senescence.

Cell Cycle Distribution Analysis of Proliferating NHOKs

The proliferative activity of the cell cultures was analysed with flow cytometric techniques. The flow cytometric measurement of propidium iodide (PI) stained DNA is shown in Fig. 6. To verify whether the PD 14.1 cells grow as exponentially growing cells, we measured cell cycle distributions of PD 10.0, 12.1, and 14.1 cells by fluorescence-activated cell sorting (FACS) analysis. The appearance of the sub-G1 phase is indicative of the occurrence of apoptosis. Percentage of cells in sub-G1/G0 fraction (0.17%, 0.33%, and 0.58%) was extremely low in cells at PD 10.0, 12.1, and 14.1 (Fig. 6), suggesting that PD 14.1 cells are considered as exponentially growing cells. Cell cycle phases were similar to different PD (Fig. 6).

Gene Expression Profiling of NHOKs via DNA Microarray

The differential gene expression profiling was performed between rapidly proliferating cells (PD 14.1) and replicative senescent cells (PD 21.6) by DNA microarray analysis.

Using the Affymetrix Human Genome U133 Plus 2.0 Array, the expression level of more than 47,000 transcripts and including approximately 38,500 characterized human genes. The data was imported into GeneSpring GX software for the identification of different state of activation or repression in the cells. These identified genes were categorized into distinct gene groups based on their known functions as shown in Table 10. Statistically significant ($p < 0.05$) differences were further reduced using the selection criteria cutoff (> 2-fold difference). As a result, 1,247 genes were upregulated, and 1,219 genes were downregulated compare to terminally differentiated and senescent (PD 21.6) NHOKs versus exponentially replicating (PD 14.1) NHOKs. Transcripts of genes involved in cellular movement, cellular differentiation, cell cycle regulation, chemokines and inflammatory factors were up-regulated in PD 21.6 cells. The expression of a subset of genes implicated in cellular proliferation was decreased in PD 21.6 cells, together with a reduction in angiogenesis-related gene expression (Table 10).

Ingenuity Analysis

To further refine the significance of the altered genes identified in senescent stage of up-regulated gene expression data, we performed network analysis using the IPA. These networks indicated functional relationships among gene products based on known interactions reported in the publications. A network was defined as known biological pathways between the uploaded predicted targets (called focus genes) and other interacting molecules produced from the Ingenuity knowledge base. The top five genetic networks

(Table 1) were identified by functional network analysis using the IPA. In particular, these networks were associated with cellular movement, development and function, cellular growth and proliferation and apoptosis. Table 1 shows these cellular functions. The focus molecules that were associated with these networks were IL-1β, S100A8, S100A9, MMP1, MMP9, and IL-8 (Fig. 7). The expression levels of the genes within these networks were confirmed by quantitative real-time RT-PCR and found similar results compared with microarray analysis data in human oral keratinocytes in response to the serial subculture (Fig. 8a-e).

Confirmation of High Levels of Marker Genes Associated with Senescence in Terminally Differentiated NHOKs via Real Time RT-PCR

Among the genetic networks identified, we focused on the cellular differentiation and senescence. Focus genes identified by the IPA program were associated with cellular movement and potential targets of the differentiation. We chose to evaluate the expression of IL-1β, S100A8, S100A9, MMP1, MMP9, and IL-8; these genes were potential target genes for terminal differentiation or replicative senescence of human oral keratinocytes. To confirmed that IL-1β, S100A8, S100A9, MMP1, MMP9, and IL-8, real-time RT-PCR was performed. These genes mRNA expression was significantly increased in replicative senescent versus exponentially replicating cells, while expression of VEGF was decreased

between the groups (Table 1, Fig. 8a-e). In order to validate the results obtained from IPA, we measured the expression of some selected genes. As shown in Fig. 8a-e for each of the examined genes, the real-time RT-PCR results similar the expression levels for these genes assessed by microarray analysis.

Induction of Cellular Senescence by IL-1β in Exponentially Growing NHOKs

To determine the molecules involved in the regulation of cellular senescence by IL-1β induction, exponentially growing NHOKs (PD 14.1) were treated with human recombinant IL-1β (10 ng/ml) for 12-96 hours. Steady-state levels of IL-1β, S100A8, S100A9, MMP1, MMP9, and IL-8 mRNAs derived from exponentially growing oral keratinocytes were consistently up-regulated in the presence of IL-1β, as determined by real-time RT-PCR analysis (Fig. 9a). VEGF mRNA expression was up-regulated after 72 hour of incubation with IL-1β, but it was significantly decreased in the long exposure (96 hour) of IL-1β (Fig. 9a).

Protection of Cellular Transformation by IL-1β Neutralizing Antibody in Senescing NHOKs

To identify the function of IL-1β in the protection of cellular transformation, human IL-1β/IL-1F2 neutralizing antibody (10 ng/ml) was treated for 14 days to determine the expression of inflammatory molecules in the senescent and terminally differentiating cells. The concentration used in the experiment was not toxic for the cells as judged by MTS assay (data not shown). IL-1β neutralizing antibody suppressed the senescence phenotypes caused by senescence and terminal differentiation (Fig. 9b).

Expression of Genes Associated with Ageing at Gingiva of Young and Aged Mice via Immunohistochemistry

Because terminally differentiated and senescent keratinocytes showed an increase of involucrin and $p16^{INK4A}$, we investigated whether these findings are relevant to the epithelium of young mice and old mice gingival tissues *in vivo* (Fig. 10a and 10b). We analyzed involucrin, $p16^{INK4A}$, IL-1β, DEC1 and VEGF expression in gingival tissue sections from the 2-years and 3-months old mice. Immunohistochemical staining showed robust levels of involucrin and $p16^{INK4A}$ in the 2-years old mice gingival tissues compared with that in tissues derived from 3-months old mice (Fig. 10a). Furthermore, IL-1β and DEC1 expression in young mice gingival tissues was present in the suprabasal layers of

epithelial cells, but the number of IL-1β and DEC1 positive cells in the basal layer was dramatically increased in 2-years old mice gingival tissues. In contrast, VEGF-positive cells in the basal layer was reduced in aged mice gingival tissues (Fig. 10b). Involucrin, $p16^{INK4A}$, IL-1β and DEC1 increased in the epithelium of old mice gingival tissues. These results revealed that a rise in involucrin, $p16^{INK4A}$ and IL-1β marks senescence of primary human keratinocytes *in vitro* as well as during normal aging of mice skin *in vivo*.

DISCUSSION

Primary NHOK undergo a finite number of replications during serial subcultures before entering a senescent phase, characterized by the loss of replicating potential and morphological alterations, followed by differentiation and senescence (12,27,44,61). In this study, evaluated the gene transcriptional profiles during subculture-induced cell differentiation and senescence in NHOKs. The serial subculture of primary NHOKs to the post-mitotic stage results in differentiation, as evidenced by increased involucrin and transglutaminase protein, the molecular marker of keratinocyte differentiation (12,58,61). Key characteristics of senescence are the $p16^{INK4A}$ is known to be a cellular factor responsible for the onset of senescence in normal cells (65,66). The activation of $p16^{INK4A}$ is believed to be a marker of a sustained DNA damage response and its expression is found to be increased with age (66,67,68). In this study, the level of cellular $p16^{INK4A}$ protein gradually increased with the serial subculture of primary NHOKs. The most commonly used marker is senescence associated β-galactosidase (SA-β-gal) activity, which reflects the increased lysosomal content of senescent cells (27). These results indicate that serial subculture of these primary keratinocytes induces replicative senescence. The microarray-based analysis, we demonstrated NHOKs transcriptional signatures profiling to specific molecular networks with gene expression patterns. The number of microarray datasets of 1,247 genes were differentially expressed in the oral keratinocytes in response to the serial subculture.

The greatest number of these altered genes was identified as being related to biologic pathways; growth factors, cell cycle, defense and immune cytokines, chemokines,

apoptosis, and inflammatory cytokines, suggesting that the serial subculture was able to induce a multitude of specific gene expression changes during differentiation and senescence. To examine the molecular function genetic networks, the data that we generated from the microarray was explored using ingenuity pathways analysis. The information generated from the Ingenuity knowledge base is consistent with the role of these genes in differentiation and senescence. Using the IPA tool, top five molecular networks identified in Table 1 as well as the primary molecular and cellular functions indicated in Fig. 7. The information generated from the Ingenuity knowledge base is consistent with the role of the cytokines in senescence. Therefore, we focused on the targets that are regulators of cellular proliferation with the hypothesis that an increased cytokine expression in the aging cells would be associated with differentiation and senescence.

IL-1β and IL-8 regulation of genes related to inflammation in human keratinocytes and endothelial cells (69,70,71). In this study, treatment with the human recombinant IL-1β in exponentially growing NHOKs led to premature senescence. The effect of inhibiting IL-1β was further confirmed using IL-1β neutralizing antibodies. IL-1β neutralizing antibody suppressed the senescence phenotypes caused by senescence and terminal differentiation. These results suggest that IL-1β plays an important role in the regulation of cellular senescence and might contribute to tissue or cellular aging. The highly up-regulated level of IL-1β expression during the serial subculture, recombinant human IL-1β-treated primary normal human keratinocytes, and gingival epithelium of aged mice clearly demonstrates that are induced to overcome this replicative senescence.

S100A8 is related to the photoaging and intrinsic aging of human skin (72). A recent study identifies calcified amyloid deposits in the ageing prostate originate from the pro-

inflammatory proteins S100A8/A9 and their amyloids (73). The current finding of upregulation of expression of S100A8/S100A9 in aging cells clearly suggested a novel view of the response to this serial subculture, and these genes may function *in vivo* as a major barrier against the replicative senescence.

Upregulation of MMP1 (matrix metalloproteinase-1) contributes to inflammatory cell intimal infiltration, plaque instability and rupture and is correlate with increased total plaque burden (74,75,76). Metalloproteinase are also implicated in multiple phases of atherosclerosis (77).

A significant transcriptional change is also observed with VEGF expression in aging cells. Cells from old animals express significantly lower levels of VEGF (78). Downregulation of VEGF and upregulation of p16 occur in aged cells (79). VEGF secretion of cells from aged mice is also decreased (80). Therefore, it is likely that a decreased VEGF expression in the aging cells may be linked with senescence.

DEC1 transcription factor, has been shown to play a role in the cell cycle regulation (79), differentiation (81), and apoptosis (79) in response to extracellular stimuli. DEC1 is induced by DNA damage in a p53-dependent manner and mediates p53-dependent cell cycle arrest and senescence (82). In the present study, an increased DEC1 expression with aging is reflective of a reduced proliferation capacity of the cells, suggesting that inhibition of ID1 expression is a mechanism by which DEC1 inhibits cell proliferation and promotes premature senescence.

In conclusion, the present study provided a comprehensive gene expression profile of primary NHOKs that accompanied subculture-induced cell differentiation and senescence. In addition, this study demonstrated that while the aging cells resulted in a multitude of

specific gene expression changes, there appeared to be some targeted biological pathways that were more selectively altered and could provide some guidance for further understanding the differentiation and senescence leading to the pathogenesis of aging

REFERENCES

1. Blanpain C, Fuchs E. Epidermal homeostasis: a balancing act of stem cells in the skin. Nat Rev Mol Cell Biol. 2009;10:207-217.
2. Simpson CL, Patel DM, Green KJ. Deconstructing the skin: cytoarchitectural determinants of epidermal morphogenesis. Nat Rev Mol Cell Biol. 2011;12:565-580.
3. Jones PH, Harper S, Watt FM. Stem cell patterning and fate in human epidermis. Cell. 1995;80:83-93.
4. Lampe MA, Williams ML, Elias PM. Human epidermal lipids: characterization and modulations during differentiation. J Lipid Res. 1983;24:131-140.
5. Fukuyama K, Kakimi S, Epstein WL. Detection of a fibrous component in keratohyalin granules of newborn rat epidermis. J Invest Dermatol. 1980;74:174-180.
6. Sun TT, Green H. Keratin filaments of cultured human epidermal cells. Formation of intermolecular disulfide bonds terminal differentiation. J Biol Chem. 1978;253:2053-2060.
7. DeLeo VA, Altman E, Christiano A, et al. Structure, function, and immunology of the skin. Omea mea. 1998;1-10.
8. Carrel A, Burrows MT. Cultivation of adult tissues and organs outside of the body. JAMA. 1910;55:1379-1381.
9. Lauer G, Otten JE, Von Specht BU, Schilli W. Cultured gingival epithelium. A possible suitable material for pre-prosthetic surgery. J Craniomaxillofac Surg. 1991;19:21-26.
10. Klingbeil MF, Herson MR, Cristo EB, et al. Comparison of two cellular harvesting methods for primary human oral culture of keratinocytes. Cell Tissue Bank.

2009;10:197-204.

11. Daniels JT, Kearney JN, Ingham E. Human keratinocyte isolation and cell culture: a survey of current practices in the UK. Burns. 1996;22:35-39.
12. Min BM, Woo KM, Lee G, et al. Terminal differentiation of normal human oral keratinocytes is associated with enhanced cellular TGF-beta and phospholipase C-gamma1 levels and apoptotic cell death. Exp Cell Res. 1999;249:377-385.
13. Candi E, Schmidt R, Melino G. The cornified envelope: a model of cell death in the skin. Nat Rev Mol Cell Biol. 2005;6:328-340.
14. Kalinin AE, Kajava AV, Steinert PM. Epithelial barrier function: assembly and structural features of the cornified cell envelope. Bioessays. 2002;24:789-800.
15. Fuchs E, Green H. Changes in keratin gene expression during terminal differentiation of the keratinocyte. Cell. 1980;19:1033-1042.
16. Schweizer J, Kinjo M, Fürstenberger G, Winter H. Sequential expression of mRNA-encoded keratin sets in neonatal mouse epidermis: basal cells with properties of terminally differentiating cells. Cell. 1984;37:159-170.
17. Roop DR, Krieg TM, Mehrel T, et al. Transcriptional control of high molecular weight keratin gene expression in multistage mouse skin carcinogenesis. Cancer Res. 1988;48:3245-3252.
18. Byrne C, Tainsky M, Fuchs E. Programming gene expression in developing epidermis. Development. 1994;120:2369–2383.
19. Simon M, Green H. Participation of membrane-associated proteins in the formation of the cross-linked envelope of the keratinocyte. Cell. 1984;36:827-834.
20. Dale BA, Holbrook KA, Kimball JR, et al. Expression of epidermal keratins and

filaggrin during human fetal skin development. J Cell Biol. 1985;101:1257-1269.

21. Hohl D, Lichti U, Breitkreutz D, et al. Transcription of the human loricrin gene *in vitro* is induced by calcium and cell density and suppressed by retinoic acid. J Invest Dermatol. 1991;96:414-418.
22. Magnaldo T, Bernerd F, Asselineau D, Darmon M. Expression of loricrin is negatively controlled by retinoic acid in human epidermis reconstructed *in vitro*. Differentiation. 1992;49:39-46.
23. Serre G, Mils V, Haftek M, et al. Identification of late differentiation antigens of human cornified epithelia, expressed in re-organized desmosomes and bound to cross-linked envelope. J Invest Dermatol. 1991;97:1061-1072.
24. Flaxman BA, Lutzner MA, Scott EJ van. Cell maturation and tissue organization in epithelial outgrowths from skin and buccal mucosa *in vitro*. J Invest Dermatol. 1967;49:322–332.
25. Doran TI, Vidrich A, Sun T-T. Intrinsic and extrinsic regulation of the differentiation of skin, corneal and esophageal epithelial cells. Cell. 1980;22:17–25.
26. Erp PEJ van, Bergers M, Grood RM, et al. Fucosyl glycopeptide profiles of keratinocytes from various epithelial tissues of the rabbit in relation to differentiation *in vivo* and *in vitro*. J Invest Dermatol. 1984;83:359–362.
27. Dimri GP, Lee X, Basile G, et al. A biomarker that identifies senescent human cells in culture and in aging skin *in vivo*. Proc Natl Acad Sci USA. 1995;92:9363-9367.
28. Bodnar AG, Ouellette M, Frolkis M, et al. Extension of life-span by introduction of telomerase into normal human cells. Science. 1998;279:349-352.
29. Watters D, Kedar P, Spring K, et al. Localization of a portion of extranuclear ATM to

peroxisomes. J. Biol. Chem.1999;274:34277-34282.

30. Parkinson EK, Newbold RF, Keith WN. The genetic basis of human keratinocyte immortalisation in squamous cell carcinoma development: the role of telomerase reactivation. Eur J Cancer. 1997;33:727-734.
31. Stanulis-Praeger BM. Cellular senescence revisited: a review. Mech Ageing Dev. 1987;38:1-48.
32. Cristofalo VJ, Pignolo RJ. Replicative senescence of human fibroblast-like cells in culture. Physiol Rev. 1993;73:617-638.
33. Chiu CP1, Harley CB. Replicative senescence and cell immortality: the role of telomeres and telomerase. Proc Soc Exp Biol Med. 1997;214:99-106.
34. Shay JW, Wright WE. Telomeres and telomerase: implications for cancer and aging. Radiat Res. 2001;155:188-193.
35. Campisi J1, Kim SH, Lim CS, Rubio M. Cellular senescence, cancer and aging: the telomere connection. Exp Gerontol. 2001;36:1619-1637.
36. Chan SW, Chang J, Prescott J, Blackburn EH. Altering telomere structure allows telomerase to act in yeast lacking ATM kinases. Curr Biol. 2001;11:1240-1250.
37. Chen Z, Trotman LC, Shaffer D, et al. Crucial role of p53-dependent cellular senescence in suppression of Pten-deficient tumorigenesis. Nature. 2005;436:725-730.
38. Blasco MA. Telomeres and human disease: ageing, cancer and beyond. Nat Rev Genet. 2005;6:611-622.
39. De Lange T. Shelterin: the protein complex that shapes and safeguards human telomeres. Genes Dev. 2005;19:2100-2110.
40. Blackburn EH. Structure and function of telomeres. Nature. 1991;350:569-573.

41. D'Adda di Fagagna F. Living on a break: Cellular senescence as a DNA-damage response. Nat Rev Cancer 2008;8:512–522.
42. Beckman KB, Ames BN. The free radical theory of aging matures. Physiol Rev. 1998;78:547–581.
43. Kregel KC, Zhang HJ. An integrated view of oxidative stress in aging: basic mechanisms, functional effects, and pathological considerations. Am J Physiol Regul Integr Comp Physiol. 2007;292:18-36.
44. Baek JH, Lee G, Kim SN, et al. Common genes responsible for differentiation and senescence of human mucosal and epidermal keratinocytes. Int J Mol Med. 2003;12:319-325.
45. Bazarov AV, Van Sluis M, Hines WC, et al. p16(INK4a)-mediated suppression of telomerase in normal and malignant human breast cells. Aging Cell. 2010;9:736-746.
46. Coppé JP, Rodier F, Patil CK, et al. Tumor suppressor and aging biomarker p16(INK4a) induces cellular senescence without the associated inflammatory secretory phenotype. J Biol Chem. 2011;286:36396-36403.
47. Rheinwald JG, Hahn WC, Ramsey MR, et al. A two-stage, p16INK4A- and p53-dependent keratinocyte senescence mechanism that limits replicative potential independent of telomere status. Mol Cell Biol. 2002;22:5157-5172.
48. Debacq-Chainiaux F, Erusalimsky JD, Campisi J, Toussaint O. Protocols to detect senescence-associated beta-galactosidase (SA-betagal) activity, a biomarker of senescent cells in culture and *in vivo*. Nat Protoc. 2009;4:1798-1806.
49. Davalos AR, Coppe JP, Campisi J, Desprez PY. Senescent cells as a source of inflammatory factors for tumor progression. Cancer Metastasis Rev. 2010;29:273-283.

50. Hayflick L. The limited *in vitro* lifetime of human diploid cell strains. Exp Cell Res. 1965;37:614-636.
51. Noordewier MO, Warren PV. Gene expression microarrays and the integration of biological knowledge. Trends Biotechnol. 2001;19:412-415.
52. De Magalhães JP, Curado J, Church GM. Meta-analysis of age-related gene expression profiles identifies common signatures of aging. Bioinformatics. 2009;25:875-881.
53. Liu D, Sartor MA, Nader GA, et al. Microarray analysis reveals novel features of the muscle aging process in men and women. J Gerontol A Biol Sci Med Sci. 2013;68:1035-1044.
54. Ashburner M, Ball CA, Blake JA, et al. Gene ontology: tool for the unification of biology. The Gene Ontology Consortium. Nat Genet. 2000;25:25-29.
55. Hall JG, Kiefer J. Arthrogryposis as a Syndrome: Gene Ontology Analysis. Mol Syndromol. 2016;7:101-109.
56. Minty F, Thurlow JK, Harrison PR, et al. Telomere dysfunction in human keratinocytes elicits senescence and a novel transcription profile. Exp Cell Res. 2008;314:2434-2447.
57. Di Cunto F, Topley G, Calautti E, et al. Inhibitory function of p21Cip1/WAF1 in differentiation of primary mouse keratinocytes independent of cell cycle control. Science. 1998;280:1069-1072.
58. Maruoka Y, Harada H, Mitsuyasu T, et al. Keratinocytes become terminally differentiated in a process involving programmed cell death. Biochem Biophys Res Commun. 1997;238:886-890.
59. Stein GH, Dulic V. Origins of G1 arrest in senescent human fibroblasts. Bioassays. 1995;17:537-543.

60. Larjava H. Expression of beta1 integrins in normal human keratinocytes. Am J Med Sci. 1991;301:63-68.
61. Kang MK, Guo W, Park NH. Replicative senescence of normal human oral keratinocytes is associated with the loss of telomerase activity without shortening of telomeres. Cell Growth Differ. 1998;9:85-95.
62. Kim RH, Lieberman MB, Lee R, et al. Bmi-1 extends the life span of normal human oral keratinocytes by inhibiting the TGF-beta signaling. Exp Cell Res. 2010;316:2600-2608.
63. Cogger VC, Svistounov D, Warren A, et al. Liver aging and pseudocapillarization in a Werner Syndrome mouse model. J Gerontol A Biol Sci Med Sci. 2014;69:1076-1086.
64. Oh JE, Kook JK, Min BM. βig-h3 induces keratinocyte differentiation via modulation of involucrin and transglutaminase expression through the integrin α3β1 and the phosphatidylinositol 3-kinase/Akt signaling pathway. J Biol Chem. 2005;280:21629-21637.
65. Hara E, Smith R, Parry D, et al. Regulation of p16CDKN2 expression and its implications for cell immortalization and senescence. Mol Cell Biol. 1996;16:859-867.
66. Loughran O, Malliri A, Owens D, et al. Association of CDKN2A/p16INK4A with human head and neck keratinocyte replicative senescence: relationship of dysfunction to immortality and neoplasia. Oncogene. 1996;13:561-568.
67. Alcorta DA, Xiong Y, Phelps D, et al. Involvement of the cyclin-dependent kinase inhibitor p16INK4a in replicative senescence of normal human fibroblasts. Proc Natl Acad Sci U S A. 1996;93:13742-13747.
68. Uhrbom L, Nister M, Westermark B. Induction of senescence in human malignant

glioma cells by p16INK4A. Oncogene. 1997;15:505-514.

69. Green HF, Treacy E, Keohane AK, et al. A role for interleukin-1beta in determining the lineage fate of embryonic rat hippocampal neural precursor cells. Mol Cell Neurosci. 2012;49:311-321.
70. Koo JW, Duman RS. IL-1β is an essential mediator of the antineurogenic and anhedonic effects of stress. Proc Natl Acad Sci U S A. 2008;105:751-756.
71. Kuzumaki N, Ikegami D, Imai S, et al. Enhanced IL-1beta production in response to the activation of hippocampal glial cells impairs neurogenesis in aged mice. Synapse. 2010;64:721-728.
72. Lee YM, Kim YK, Eun HC, et al. Changes in S100A8 expression in UV-irradiated and aged human skin *in vivo*. Arch Dermatol Res. 2009;301:523-529.
73. Yanamandra K, Alexeyev O, Zamotin V, et al. Amyloid formation by the pro-inflammatory S100A8/A9 proteins in the ageing prostate. PLoS One. 2009;4:e5562.
74. Hanemaaijer R, Koolwijk P, le Clercq L, de Vree WJ, van Hinsbergh VW. Regulation of matrix metalloproteinase expression in human vein and microvascular endothelial cells. Effects of tumour necrosis factor alpha, interleukin 1 and phorbol ester. Biochem J. 1993;296:803–809.
75. Nikkari ST, O'Brien KD, Ferguson M, Hatsukami T, Welgus HG, Alpers CE, et al. Interstitial collagenase (MMP-1) expression in human carotid atherosclerosis. Circulation. 1995;92:1393–1398.
76. Lehrke M, Greif M, Broedl UC, Lebherz C, Laubender RP, Becker A, et al. MMP-1 serum levels predict coronary atherosclerosis in humans. Cardiovascular diabetology. 2009;8:50.

77. Dollery CM, Libby P. Atherosclerosis and proteinase activation. Cardiovasc Res. 2006;69:625–635.
78. Asumda FZ, Chase PB. Age-related changes in rat bone-marrow mesenchymal stem cell plasticity. BMC Cell Biol. 2011;12:44.
79. Li Y, Zhang H, Xie M, et al. Abundant expression of Dec1/stra13/sharp2 in colon carcinoma: its antagonizing role in serum deprivation-induced apoptosis and selective inhibition of procaspase activation. Biochem J. 2002;367:413-422.
80. Wilson A, Shehadeh LA, Yu H, et al. Age-related molecular genetic changes of murine bone marrow mesenchymal stem cells. BMC Genomics. 2010;11:229.
81. Seimiya M, Wada A, Kawamura K, et al. Impaired lymphocyte development and function in Clast5/Stra13/DEC1-transgenic mice. Eur J Immunol. 2004;34:1322-1332.
82. Qian Y, Zhang J, Yan B, et al. DEC1, a basic helix-loop-helix transcription factor and a novel target gene of the p53 family, mediates p53-dependent premature senescence. J Biol Chem. 2008;283:2896-2905.

Table 1. Functional networks in the exponentially growing (PD 14.1) and terminally differentiated and replicative senescent (PD 21.6) NHOKs

Network	Focus genes[a]	Score[b]	Top functions
1	↓*ALDH7A1*, ↑***ANGPTL4***, ↓*ASS*, ↓*BAMBI*, ↓*CBS*, ↓***CEBPG***, ↑***DCN***, ↓***DDIT3***, ↓***FST***, ↑*GM2A*, ↓*HMGN2*, ↓*HPSE*, ↑***IL-1B***, ↑*IL1F5*, ↓*IL1RAP*, ↑***INHBA***, ↓*JDP2*, ↑***KLF11***, ↑*MARCKSL1*, ↑***MMP3***, ↑*OAS2*, ↓*OGG1*, ↑***PGF***, ↑*PIM3*, ↓*PPP1R14A*, ↓*PROCR*, ↑*RNASE7*, ↑***S100A8***, ↑***S100A9***, ↑*SAA1*, ↓*SLC11A2*, ↑*SLC20A1*, ↓*SLC37A4*, ↑***SOD2***, ↑*UGCG*	36	Cell death, Renal and urological disease, Cancer
2	↑*ADAMTS1*, ↑*CLDN1*, ↑***CTGF***, ↑***CYR61***, ↑***DDR1***, ↑*DUSP4*, ↓*EMP2*, ↓*ETV4*, ↓*ETV5*, ↓*FBLN1*, ↓*FGF2*, ↑*FN1*, ↓*GART*, ↓*HYOU1*, ↓*FBLN1*, ↓*FGF2*, ↑*FN1*, ↓*GART*, ↓*HYOU1*, ↓*IGFBP2*, ↑***ITGA2***, ↑*ITGA5*, ↑*ITGB6*, ↑*ITGB8*, ↑*MFAP5*, ↑***MMP1***, ↑***MMP14***, ↓*NUP88*, ↑***S100A4***, ↑*S100A7*, ↓*SH2D2A*, ↑*SPINK1*, ↓*STK16*, ↑*TFP1*, ↑*TGM2*, ↑***TIMP2***, ↓***VEGF***, ↓***VEGFB***, ↓*VRK1*, ↓*ZNF410*	36	Cancer, Cellular movement, Cardiovascular system, Development & function
3	↑*ADAM9*, ↑*ADAM19*, ↓***AREG***, ↓*CBLC*, ↓*CDH4*, ↑*CEACAM6*, ↓*CKS2*, ↓*COL4A2*, ↑*COL5A2*, ↑*CXCL1*, ↑*CXCL5*, ↑*CXCL14*, ↑*DUSP6*, ↓*EGFR*, ↓***EREG***, ↓*ERRFI1*, ↑*GRB7*, ↓*GRB10*, ↓*GTF3A*, ↑*HBEGF*, ↑***IL-8***, ↑*IL32*, ↓*MKI67*, ↑***MMP9***, ↓*NFIB*, ↓***NRG1***, ↓*PACSIN3*, ↑***PTGS2***, ↓*RNF41*, ↑*SH3KBP1*, ↑*SLP1*, ↑*SOX4*, ↑***SPRY2***, ↓*TOM1L1*, ↓*ZNF259*	36	Cellular Growth & Proliferation, Cancer, Cellular Movement

4	*ALPΔ,* ↑***BHLHB2***, ↑***BMP2***, ↓*C18ORF37,* ↓*DEK,* ↓*EIF5A,* ↓*ELOVL6,* ↓***FOXG1B***, ↑***HES1***, ↑***ID3***, ↑*KPNB1,* ↓*MCRS1,* ↓*MGC21874,* ↓***NFATC3***, ↓***NUP98***, ↓*NUP153,* ↓*P8,* ↑***PCAF***, ↓*PPAN,* ↓*RANBP1,* ↓*RCC1* (includes EG: 1104), ↓*RUVBL1,* ↓*SITPEC,* ↓***SMAD1***, ↓*SNRPA,* ↑***SOX9***, ↓*SRRM1,* ↓*TACC3,* ↑***TGM1***, ↑*TLX2,* ↓*TPR,* ↑***TWIST1***, ↓*UPF3B,* ↓*WDR5,* ↓*ZNF423*	25	Gene expression, Cell signaling, Cellular development
5	↓*ATAD3A,* ↓*BCAT1,* ↑***BMP4***, ↓*C1ORF24,* ↓*CDCA7,* ↓*CSDE1,* ↓*DDX18,* ↓***DKK1***, ↑***E2F4***, ↑***FGF10***, ↑*FRAP1,* ↑*GATA1,* ↑*GATA2,* ↓*H2AFZ,* ↓***ID1***, ↑*ID2,* ↑***ID3***, ↓*IGF1,* ↓*LEF1,* ↓*MAX,* ↓*MINA,* ↓*MRPL12,* ↓*MTHFD1,* ↓***MYC***, ↓*NCAM1,* ↓*NFYC,* ↓***NOG***, ↑*PABPC1,* ↑*PERP,* ↓*PSAT1,* ↓*PYCR2,* ↑***SCEL***, ↓***SMARCA4***, ↓*WNT5A,* ↓*YME1L1*	8	Cellular development, Gene expression, Cell cycle

[a] Bold and underlined genes are confirmed by the real-time RT-PCR.

[b] A score of >3 was considered significant ($P < 0.001$).

Table 2. Primer sequences used for RT-PCR and real-time RT-PCR

Gene (NCBI ID)	Sequence
Involucrin (NM_005547.2)	
Forward primer	5’-GGCCACCCAAACATAAATAACCAC-3’
Reverse primer	5’-CACCTAGCGGACCCGAAATAAGT-3’
Transglutaminase (NM_000359.2)	
Forward primer	5’-CACATCCCTTACCATGGACATCTAC-3’
Reverse primer	5’-GCAGTCGTTCCACACATGGA-3’
$p16^{INK4A}$ (NM_000077.4)	
Forward primer	5’-CTCCGGAAGCTGTCGACTTC-3’
Reverse primer	5’-TTCTGCCATTTGCTAGCAGTGT-3’
GAPDH (NM_002046.4)	
Forward primer	5’-CCATCTTCCAGGAGCGAGATC-3’
Reverse primer	5’-GCCTTCTCCATGGTGGTGAA-3’

Table 3. Primer sequences used in network 1 for real-time RT-PCR

Gene (NCBI ID)	Sequences
ANGPTL4 (NM_139314.1)	
Forward primer	5’-GAAAGAGGCTGCCCGAGATGG-3’
Reverse primer	5’-GGAGACCCCTGAGGCTGGATTT-3’
CEBPG (NM_001252296.1)	
Forward primer	5’-TTGGCAGCTTAGCGTGGAA-3’
Reverse primer	5’-TTGCTGCGATATCTTGCTCATT-3’
DCN (NM_001920.3)	
Forward primer	5’-GGTGTCAGCCGGATTGTGTTCA-3’
Reverse primer	5’-AGGGGGTAGGTGCTGCTCTGTG-3’
DDIT3 (NM_004083.5)	
Forward primer	5’-GGAGCATCAGTCCCCCACTT-3’
Reverse primer	5’-GTGGGATTGAGGGTCACATCA-3’
FST (NM_006350.3)	
Forward primer	5’-GCGGGCTGGATGGGAAAAC-3’
Reverse primer	5’-ACACATGTGGAGCTGCCTGGAC-3’
IL1β (NM_000576.2)	
Forward primer	5’-GGCAGGCCGCGTCAGTTC-3’
Reverse primer	5’-AAGGGAAAGAAGGTGCTCAGGTCA-3’
INHBA (NM_002192.2)	
Forward primer	5’-AAAAGAAGGGCGGAGGTGAAGG-3’
Reverse primer	5’-CCGGCGATGAGGGTGGTCT-3’
KLF11 (NM_003597.4)	
Forward primer	5’-TGCTGTGGCCTTATCCGTACT-3’

Reverse primer	5’-AAGCTGTGCTCTGGTGGAGTTT-3’
MMP3 (NM_002422.3)	
Forward primer	5’-TACAAGGAGGCAGGCAAGACAGC-3’
Reverse primer	5’-GCCACGCACAGCAACAGTAGGA-3’
PGF (NM_002632.5)	
Forward primer	5’-GGCCTTGTCTGCTGGGAACG-3’
Reverse primer	5’-CGCTGGGGTACTCGGACACG-3’
S100A8 (NM_002964.4)	
Forward primer	5’-CTATCATCGACGTCTACCACAAGTACT-3’
Reverse primer	5’-TGAGGACACTCGGTCTCTAGCA-3’
S100A9 (NM_002965.3)	
Forward primer	5’-GGACACAAATGCAGACAAGCA-3’
Reverse primer	5’-CTCGTCACCCTCGTGCATCT-3’
SOD2 (NM_000636.2)	
Forward primer	5’-GCGCCCTGGAACCTCACATC-3’
Reverse primer	5’-CAACGCCTCCTGGTACTTCTCCTC-3’
HPRT1 (NM_000184.2)	
Forward primer	5’-GGTCAGGCAGTATAATCCAAAGA-3’
Reverse primer	5’-GGGCATATCCTACAACAAACT-3’

Table 9 for the abbreviations of genes.

Table 4. Primer sequences used in network 2 for real-time RT-PCR

Gene (NCBI ID)	Sequences
S100A4 (NM_002961.2)	
Forward primer	5’-GAAGGCCCTGGATGTGATGGTGTC-3’
Reverse primer	5’-CTCCCGGGTCAGCAGCTCCTTTAG-3’
ITGA2 (NM_002203.3)	
Forward primer	5’-AACGGGACTTTCGCATCATC-3’
Reverse primer	5’-TACTTCGGCTTTCTCATCAGGTTT-3’
VEGF (AF_022375.1)	
Forward primer	5’-ACGCTGCCGCCACCACACC-3’
Reverse primer	5’-TCTCGCCCTCCGGACCCAAAGT-3’
CTGF (NM_001901.2)	
Forward primer	5’-GGCCCAGACCCAACTATGAT-3’
Reverse primer	5’-AGGCGGCTCTGCTTCTCTA-3’
VEGFB (NM_001243733.1)	
Forward primer	5’-CTCTAGGACCTGGGCCTCTCA-3’
Reverse primer	5’-CTGCCTCCCAGTCTCCTCTTC-3’
DDR1 (NM_013993.2)	
Forward primer	5’-TGCGCTATCTGGCCACACTCAACT-3’
Reverse primer	5’-CGGCCCTGCACACGGTAATAG-3’
CYR61 (NM_001554.4)	
Forward primer	5’-ACGGCTGCGGCTGCTGTAAGGTCT-3’
Reverse primer	5’-GTGGAGCTGGCGCCGAAGTTGC-3’
TIMP2 (NM_003255.4)	
Forward primer	5’-CCAAAGCGGTCAGTGAGAAGGAAG-3’

Reverse primer	5’-CCGAGGAGGGGGCCGTGTAGATA-3’
MMP1 (NM_002421.3)	
Forward primer	5’-ATTCTACTGATATCGGGGCTTTGA-3’
Reverse primer	5’-GATGGGCTGGACAGGATTTTG-3’
MMP14 (NM_004995.2)	
Forward primer	5’-GGCCCGCCCACTCCTACCACAAG-3’
Reverse primer	5’-AAGGAGGCCAGCCAGGGGACAGAG-3’
HPRT1 (NM_000184.2)	
Forward primer	5’-GGTCAGGCAGTATAATCCAAAGA-3’
Reverse primer	5’-GGGCATATCCTACAACAAACT-3’

Table 9 for the abbreviations of genes.

Table 5. Primer sequences used in network 3 for real-time RT-PCR

Gene (NCBI ID)	Sequences
AREG (NM_001657.2)	
Forward primer	5'-CCCGGTCTCCACTCGCTCTTC-3'
Reverse primer	5'-CGGGGCTCTCATTGGTCCTTC-3'
EREG (NM_001432.2)	
Forward primer	5'-CTGTGGAGGCTGAGATGAAAACT-3'
Reverse primer	5'-TGCAATAGCCCAAAAATACTCCT-3'
IL8 (NM_000584.3)	
Forward primer	5'-TCAGAGACAGCAGAGCACACAA-3'
Reverse primer	5'-GGCCAGCTTGGAAGTCATGT-3'
MMP9 (NM_004994.2)	
Forward primer	5'-GGCACCACCACAACATCACCTATT-3'
Reverse primer	5'-CGTCACCGCGCTCCACAGT-3'
NRG1 (NM_013964.3)	
Forward primer	5'-CCTTGCCTCCCCGATTGA-3'
Reverse primer	5'-TCCCATTCTTGAACCACTTGA-3'
PTGS2 (NM_000963.2)	
Forward primer	5'-CAGCCAGACGCCCTCAGACAG-3'
Reverse primer	5'-ATGGGTGGGAACAGCAAGGATTT-3'
SPRY2 (NM_005842.2)	
Forward primer	5'-TGCACGCCTACAGGTGTGA-3'
Reverse primer	5'-AGGCACTGCTTGTCGCAGAT-3'
HPRT1 (NM_000184.2)	
Forward primer	5'-GGTCAGGCAGTATAATCCAAAGA-3'
Reverse primer	5'-GGGCATATCCTACAACAAACT-3'

Table 9 for the abbreviations of genes.

Table 6. Primer sequences used in network 4 for real-time RT-PCR

Gene (NCBI ID)	Sequences
NUP98 (NM_016320.4)	
Forward primer	5’-GCTTTGACAGATCCAAATGCTTCT-3’
Reverse primer	5’-GATTCCGGAAGAGAGGAGAGTCT-3’
TGM1 (NM_000359.2)	
Forward primer	5’-AGACTCCCGCCGGCCTGTATCC-3’
Reverse primer	5’-GGTGCTCTCGGCGGTTCTGGTC-3’
NFATC3 (NM_173165.2)	
Forward primer	5’-GCCACACCCCTATATTTCGCACAT-3’
Reverse primer	5’-CCCCTCGGCTACCTTCAGTTTCAT-3’
SOX9 (NM_000346.3)	
Forward primer	5’-GGCCAGTCCCAGCGAACG-3’
Reverse primer	5’-GAGCGGGTGATGGGCGGGTAGG-3’
BMP2 (NM_001200.2)	
Forward primer	5’-CCCCACGGAGGAGTTTATCACC-3’
Reverse primer	5’-ACGGGGAATTTCGAGTTGGCTGTT-3’
BHLHB2 (NM_003670.2)	
Forward primer	5’-GGCCCACACCCACACCAG-3’
Reverse primer	5’-TGCGGCAGAGGCGTTGAG-3’
HES1 (NM_005524.3)	
Forward primer	5’-CAGGCTGGAGAGGCGGCTAAGGTG-3’
Reverse primer	5’-GGAGGTGCCGCTGTTGCTGGTGTA-3’

SMAD1 (NM_005900.2)	
Forward primer	5’-GATACGCCCCCACCTGCTTACCTG-3’
Reverse primer	5’-GCAACCGCCTGAACATCTCCTCTG-3’
PCAF (NM_003884.4)	
Forward primer	5’-TGGCCGTGTTATTGGTGGTA-3’
Reverse primer	5’-GCCCTTGACTTGCTCATTTGA-3’
FOXG1B (NM_005249.4)	
Forward primer	5’-CGGCTCACGCTCAACGGCATCTAC-3’
Reverse primer	5’-TGGCGCGGCACCTTCACGA-3’
TWIST1 (NM_000474.3)	
Forward primer	5’-CAGCGGCACCATCCTCACACCTCT-3’
Reverse primer	5’-TGGCTGATTGGCACGACCTCTTGA-3’
ID3 (NM_002167.4)	
Forward primer	5’-AGCTCGCTCCGGAACTTGTCATC-3’
Reverse primer	5’-TCCCGGGGTCCCAGGCAGAAC-3’
HPRT1 (NM_000184.2)	
Forward primer	5’-GGTCAGGCAGTATAATCCAAAGA-3’
Reverse primer	5’-GGGCATATCCTACAACAAACTC-3’

Table 9 for the abbreviations of genes.

Table 7. Primer sequences used in network 5 for real-time RT-PCR

Gene (NCBI ID)	Sequences
BMP4 (NM_001202.3)	
Forward primer	5’-TCACAGCGGGCCAGGAAGAAGAAT-3’
Reverse primer	5’-GGCAGTCCCCATGGCAGTAGAAGG-3’
ID3 (NM_002167.4)	
Forward primer	5’-AGCTCGCTCCGGAACTTGTCATC-3’
Reverse primer	5’-TCCCGGGGTCCCAGGCAGAAC-3’
MYC (NM_002467.4)	
Forward primer	5’-CGACGCGGGGAGGCTATTCTGC-3’
Reverse primer	5’-ATCGTCGCGGGAGGCTGCTGGTTT-3’
SMARCA4 (NM_003072.3)	
Forward primer	5’-AAGGGCAAAGGCGGCACCAAGACC-3’
Reverse primer	5’-AATGCCGCCAGTGAACCCCAAGTG-3’
SCEL (NM_144777.2)	
Forward primer	5’-CACTTACTGCCGAAAACC-3’
Reverse primer	5’-TCACCCGCTTGTAGATT-3’
FGF10 (NM_004465.1)	
Forward primer	5’-TCACCAGAGGCCACCAACTC-3’
Reverse primer	5’-AGCGGACATCTCCTTGAAGGT-3’
DKK1 (NM_012242.2)	
Forward primer	5’-CCGGGTCTTTGTCGCGATGGTAGC-3’
Reverse primer	5’-AGCGGTGGGGGCAGGTTCTTGAT-3’
E2F4 (NM_001950.3)	
Forward primer	5’-GGCCTCCCCTCACCGCACAGTT-3’

Reverse primer	5’-CGAAGGCCGCAGAAAGGGAGAA-3’
NOG (NM_005450.4)	
Forward primer	5’-GCCCGGCACCCAGCGACAAC-3’
Reverse primer	5’-CGTAGTGGCCCCCGAGCAG-3’
ID1 (NM_181353.2)	
Forward primer	5’-CGACATGAACGGCTGTTACTCA-3’
Reverse primer	5’-GTCGATGACGTGCTGGAGAA-3’
HPRT1 (NM_000184.2)	
Forward primer	5’-GGTCAGGCAGTATAATCCAAAGA-3’
Reverse primer	5’-GGGCATATCCTACAACAAACT-3’

Table 9 for the abbreviations of genes.

Table 8. Primer sequences used for analysis of inflammatory genes after IL-1β treatment in real-time RT-PCR

Gene (NCBI ID)	Sequences
IL-1β (NM_000576.2)	
Forward primer	5'-GGCAGGCCGCGTCAGTTC-3'
Reverse primer	5'-AAGGGAAAGAAGGTGCTCAGGTCA-3'
S100A8 (NM_002964.4)	
Forward primer	5'-CTATCATCGACGTCTACCACAAGTACT-3'
Reverse primer	5'-TGAGGACACTCGGTCTCTAGCA-3'
S100A9 (NM_002965.3)	
Forward primer	5'-GGACACAAATGCAGACAAGCA-3'
Reverse primer	5'-CTCGTCACCCTCGTGCATCT-3'
MMP1 (NM_002421.3)	
Forward primer	5'-ATTCTACTGATATCGGGGCTTTGA-3'
Reverse primer	5'-GATGGGCTGGACAGGATTTTG-3'
MMP9 (NM_004994.2)	
Forward primer	5'-GGCACCACCACAACATCACCTATT-3'
Reverse primer	5'-CGTCACCGCGCTCCACAGT-3'
VEGF (AF_022375.1)	
Forward primer	5'-ACGCTGCCGCCACCACACC-3'
Reverse primer	5'-TCTCGCCCTCCGGACCCAAAGT-3'
IL-8 (NM_000584.3)	
Forward primer	5'-TCAGAGACAGCAGAGCACACAA-3'
Reverse primer	5'-GGCCAGCTTGGAAGTCATGT-3'
HPRT1 (NM_000184.2)	
Forward primer	5'-GGTCAGGCAGTATAATCCAAAGA-3'
Reverse primer	5'-GGGCATATCCTACAACAAACT-3'

Table 9 for the abbreviations of genes.

Table 9. The abbreviation of genes

Symbol	Description
Network 1	
ANGPTL4	Angiopoietin-related protein 4
CEBPG	CCAAT/enhancer-binding protein gamma
DCN	Decorin
DDIT3	DNA damage-inducible transcript 3
FST	Follistatin
IL-1B	Interleukin-1 beta
INHBA	Inhibin, beta A
KLF11	Krueppel-like factor 11
MMP3	Matrix Metalloproteinase-3
PGF	Placental growth factor
S100A8	S100 Calcium Binding Protein A8
S100A9	S100 calcium binding protein A9
SOD2	Superoxide dismutase 2
Network 2	
ITGA2	Integrin, alpha 2
CTGF	Connective tissue growth factor
VEGF	Vascular endothelial growth factor
CYR61	Cysteine-rich angiogenic inducer 61
MMP1	Matrix metalloproteinase-1
MMP14	Matrix metalloproteinase-14
S100A4	S100 calcium binding protein A4
DDR1	Discoidin domain receptor tyrosine kinase 1
TIMP2	TIMP metallopeptidase inhibitor 2
VEGFB	Vascular endothelial growth factor B
Network 3	
AREG	Amphiregulin
EREG	Epiregulin
IL-8	Interleukin-8

MMP9	Matrix Metalloproteinase-9
NRG1	Neuregulin 1
PTGS2	Prostaglandin-endoperoxide synthase 2
SPRY2	Sprouty homolog 2

Network 4

BHLHB2	Basic helix-loop-helix B2
ID3	Inhibitor of DNA binding 3
BMP2	Bone morphogenetic protein 2
FOXG1B	Forkhead box protein G1
HES1	Hairy and enhancer of split-1
NFATC3	Nuclear factor of activated T-cells, cytoplasmic 3
SMAD1	SMAD family member 1
SOX9	SRY (sex determining region Y)-box 9
TGM1	Transglutaminase-1
TWIST1	Twist-related protein 1
NUP98	Nuclear pore complex protein
PCAF	P300/CBP-associated factor

Network 5

BMP4	Bone morphogenetic protein 4
E2F4	E2F transcription factor 4
DKK1	Dickkopf-related protein 1
ID3	Inhibitor of DNA binding 3
FGF10	Fibroblast growth factor 10
SCEL	Sciellin
SMARCA4	SWI/SNF related, matrix associated, actin dependent regulator of chromatin, subfamily a, member 4
MYC	v-myc myelocytomatosis viral oncogene homolog
NOG	Noggin
ID1	Inhibitor of DNA binding

Table 10. Upregulated and downregulated genes in human oral keratinocytes in response to serial subculture (DNA microarray)

UPREGULATED GENES

Gene ontology/genes	Symbol	GeneBank ID	Fold change
Cell growth			
epithelial membrane protein1	EMP1	NM_001423	6.2
Kruppel-like factor 6	KLF6	NM_001300	2.9
Cell cycle			
interleukin 8	IL8	NM_000584	14.6
p16	CDKN2A	NM_000077	9.8
cyclin G2	CCNG2	NM_004354	5.6
p57	DCKN1C	NM_000076	4.5
retinoblastoma 1	RB1	NM_000321	3.6
cyclin D1	CCND1	NM_053056	3.4
p15	CDKN2B	NM_004936	3.4
dual specificity phosphatase 1	DUSP1	NM_004417	3.1
p19	CDKN2D	NM_001800	2.6
Cell death			
interleukin 6	IL6	NM_000600	4.3
interleukin 1, beta	IL1B	NM_000576	3.0
tumor necrosis factor	TNF	NM_000594	2.8
Growth factor activity			
fibroblast growth factor 5	FGF5	NM_004464	15.7
chemokine(C-X-C motif) ligand 12	CXCL12	NM_000609	7.2
bone morphogenetic protein 6	BMP6	NM_001718	6.1
chemokine(C-X-C motif) ligand 1	CXCL1	NM_001511	5.8
bone morphogenetic protein 2	BMP2	NM_001200	2.3
Cell adhesion			
intercellular adhesion molecule 1	ICAM1	NM_000201	162.9
periostin	POSTN	NM_006475	30.5
chemokine(C-C motif) ligand 5	CCL5	NM_002985	27.8
fibronectin 1	FN1	NM_002026	23.6

versican	VCAN	NM_004385	19.7
claudin 1	CLDN1	NM_021101	11.7
connective tissue growth factor	CTGF	NM_001901	11.4
collagen, type VI, alpha 2	COL6A2	NM_00184	9.8
claudin 4	CLDN4	NM_001305	7.4
Cell surface receptor linked signaling pathway			
paired box gene 8	PAX8	NM_003466	50.2
toll-like receptor 2	TLR2	NM_003264	22.9
transforming growth factor beta receptor I	TGF-β1	NM_004612	8.0
defensin, beta 1	DEFB1	NM_005218	7.3
chemokine(C-X-C motif) ligand 10	CXCL10	NM_001565	6.4
bone morphogenetic protein 6	BMP6	NM_001718	6.1
chemokine(C-X-C motif) ligand 1	CXCL1	NM_001511	5.8
interleukin 6	IL6	NM_000600	4.3
signal transducer and activator of transcription 4	STAT4	NM_003151	2.8
Intracellular signaling pathway			
dual specificity phosphatase 10	DUSP10	NM_007207	17.9
interleukin 8	IL8	NM_000584	14.6
chemokine(C-X-C motif) ligand 1	CXCL1	NM_001511	5.8
interleukin-1 receptor-associated kinase 2	IRAK2	NM_001570	4.1
toll-like receptor 1	TLR1	NM_003263	3.8
cyclin D1	CCND1	NM_053056	3.4
dual specificity phosphatase 6	DUSP6	NM_001946	2.1
Cytokine activity			
interleukin 33	IL33	NM_033439	44.0
chemokine(C-X-C motif) ligand 5	CXCL5	NM_002994	29.7
chemokine(C-C motif) ligand 5	CCL5	NM_002985	27.8
interleukin 8	IL8	NM_000584	14.6
chemokine(C-X-C motif) ligand 12	CXCL12	NM_000609	7.2
chemokine(C-X-C motif) ligand 10	CXCL10	NM_001565	6.4
bone morphogenetic protein 6	BMP6	NM_001718	6.1
chemokine(C-X-C motif) ligand 1	CXCL1	NM_001511	5.8
chemokine(C-X-C motif) ligand 14	CXCL14	NM_004887	5.7
interleukin 32	IL32	NM_004221	4.6

interleukin 6	IL6	NM_000600	4.3
chemokine(C-C motif) ligand 27	CCL27	NM_006664	3.2
chemokine(C-C motif) ligand 20	CCL20	NM_004591	3.1
interleukin 24	IL24	NM_006850	2.8
tumor necrosis factor	TNF	NM_000594	2.8
interleukin 20	IL20	NM_018724	2.8
chemokine(C-X-C motif) ligand 11	CXCL11	NM_005409	2.5
bone morphogenetic protein 2	BMP2	NM_001200	2.2
chemokine(C-X-C motif) ligand 2	CXCL2	NM_002089	2.1
Proteolysis			
matrix metallopeptidase 12	MMP12	NM_002426	36.7
matrix metallopeptidase 10	MMP10	NM_002425	7.5
kallikrein-related peptidase 7	KLK7	NM_005046	7.0
matrix metallopeptidase 9	MMP9	NM_004994	4.8
matrix metallopeptidase 3	MMP3	NM_002422	4.7
cathepsin S	CTSS	NM_004079	4.2
plasminogen activator urokinase	PLAU	NM_002658	4.1
matrix metallopeptidase 1	MMP1	NM_002421	4.0
kallikrein-related peptidase 13	KLK13	NM_015596	3.7
matrix metallopeptidase 28	MMP28	NM_024302	3.7
matrix metallopeptidase 14	MMP14	NM_004995	3.6
cathepsin L2	CTSL2	NM_001333	3.5
kallikrein-related peptidase 8	KLK8	NM_007196	3.3
cathepsin B	CTSB	NM_001908	3.3
matrix metallopeptidase 2	MMP2	NM_004530	2.9
cathepsin H	CTSH	NM_004390	2.8
cathepsin F	CTSF	NM_003793	2.6
Apoptosis			
cyclin-dependent kinase inhibitor 2A	CDKN2A	NM_000077	9.8
interleukin 6	IL6	NM_000600	4.3
interleukin 1, beta	IL1B	NM_000576	3.0
interleukin 24	IL24	NM_006850	2.8
Response to stress			
S100 calcium binding protein A7	S100A7	NM_002963	181.7
chemokine(C-X-C motif) ligand 5	CXCL5	NM_002994	29.7

chemokine(C-C motif) ligand 5	CCL5	NM_002985	27.8
fibronectin 1	FN1	NM_002026	23.6
toll-like receptor 2	TLR2	NM_003264	22.9
dual specificity phosphatase 10	DUSP10	NM_007207	17.9
interleukin 8	IL8	NM_000584	14.6
S100 calcium binding protein A12	S100A12	NM_005621	9.7
defensin, beta 1	DEFB1	NM_005218	7.3
chemokine(C-X-C motif) ligand 12	CXCL12	NM_000609	7.2
chemokine(C-X-C motif) ligand 10	CXCL10	NM_001565	6.4
S100 calcium binding protein A9	S100A9	NM_002965	6.2
chemokine(C-X-C motif) ligand 1	CXCL1	NM_001511	5.8
defensin, beta 4	DEFB4	NM_004942	5.8
chemokine(C-X-C motif) ligand 14	CXCL14	NM_004887	5.7
interleukin 6	IL6	NM_000600	4.3
superoxide dismutase 2, mitochondrial	SOD2	NM_000636	3.9
toll-like receptor 1	TLR1	NM_003263	3.8
S100 calcium binding protein A8	S100A8	NM_002964	3.4
chemokine(C-C motif) ligand 20	CCL20	NM_004591	3.1
dual specificity phosphatase 1	DUSP1	NM_004417	3.1
interleukin 1, beta	IL1B	NM_000576	3.0
heat shock 27kDa protein 1	HSPB1	NM_001540	2.8
chemokine(C-X-C motif) ligand 11	CXCL11	NM_005409	2.5
chemokine(C-X-C motif) ligand 2	CXCL2	NM_002089	2.1
Inflammatory response			
chemokine(C-X-C motif) ligand 5	CXCL5	NM_002994	29.7
chemokine(C-C motif) ligand 5	CCL5	NM_002985	27.8
toll-like receptor 2	TLR2	NM_003264	22.9
interleukin 8	IL8	NM_000584	14.6
S100 calcium binding protein A12	S100A12	NM_005621	9.7
chemokine(C-X-C motif) ligand 12	CXCL12	NM_000609	7.2
chemokine(C-X-C motif) ligand 10	CXCL10	NM_001565	6.4
S100 calcium binding protein A9	S100A9	NM_002965	6.2
chemokine(C-X-C motif) ligand 1	CXCL1	NM_001511	5.8
chemokine(C-X-C motif) ligand 14	CXCL14	NM_004887	5.7
interleukin 6 (interferon, beta 2)	IL6	NM_000600	4.3
toll-like receptor 1	TLR1	NM_003263	3.8
S100 calcium binding protein A8	S100A8	NM_002964	3.4

chemokine(C-C motif) ligand 20	CCL20	NM_004591	3.1
interleukin 1, beta	IL1B	NM_000576	3.0
chemokine(C-X-C motif) ligand 11	CXCL11	NM_005409	2.5
chemokine(C-X-C motif) ligand 2	CXCL2	NM_002089	2.1
chemokine(C-C motif) receptor 2	CCL2	NM_000647	2.0
Immune response			
S100 calcium binding protein A7	S100A7	NM_002963	181.7
chemokine(C-X-C motif) ligand 5	CXCL5	NM_002994	29.7
chemokine (C-C motif) ligand 5	CCL5	NM_002985	27.8
toll-like receptor 2	TLR2	NM_003264	22.9
interleukin 8	IL8	NM_000584	14.6
defensin, beta 1	DEFB1	NM_005218	7.3
chemokine(C-X-C motif) ligand 12	CXCL12	NM_000609	7.2
chemokine(C-X-C motif) ligand 10	CXCL10	NM_001565	6.4
chemokine(C-X-C motif) ligand 1	CXCL1	NM_001511	5.8
defensin, beta 4	DEFB4	NM_004942	5.8
chemokine(C-X-C motif) ligand 14	CXCL14	NM_004887	5.7
interleukin 6 (interferon, beta 2)	IL6	NM_000600	4.3
toll-like receptor 1	TLR1	NM_003263	3.8
chemokine (C-C motif) ligand 27	CCL27	NM_006664	3.2
chemokine (C-C motif) ligand 20	CCL20	NM_004591	3.1
interleukin 1, beta	IL1B	NM_000576	3.0
Multicellular organismal development			
S100 calcium binding protein A7	S100A7	NM_002963	181.7
Decorin	DCN	NM_001920	59.3
paired box gene 8	PAX8	NM_003466	50.2
cystatin E/M	CST6	NM_001323	19.7
versican	VCAN	NM_004385	19.7
paired box gene 4	PAX4	NM_006193	17.2
fibroblast growth factor 5	FGF5	NM_004464	15.7
periostin	POSTN	NM_006475	12.2
S100 calcium binding protein A4	S100A4	NM_002961	11.3
Cbp/p300-interacting transactivator	CITED2	NM_006079	11.3
chemokine(C-X-C motif) ligand 10	CXCL10	NM_001565	6.4
runt-related transcription factor 1	RUNX1	NM_001754	5.6
hairy and enhancer of split 1	HES1	NM_005524	5.3

pim-1 oncogene	PIM1	NM_002648	4.7
early growth response 3	EGR3	NM_004430	4.1
SRY(sex determining region Y)-box 9	SOX9	NM_000346	3.7
inhibitor of DNA binding 3	ID3	NM_002167	3.0
high-mobility group box 3	HMGB3	NM_005342	3.0
SRY(sex determining region Y)-box 4	SOX4	NM_003107	2.6
frizzled homolog 7	FZD7	NM_003507	2.4
twist homolog 1	TWIST1	NM_000474	2.2
transglutaminase 1	TGM1	NM_000359	2.1

Table 10. Upregulated and downregulated genes in human oral keratinocytes in response to serial subculture (DNA microarray)

DOWNREGULATED GENES

Gene ontology/genes	Symbol	GeneBank ID	Fold change
Cell cycle			
cell division cycle 20	CDC20	NM_001255	0.03
cyclin dependent kinase inhibitor 3	CDKN3	NM_005192	0.04
cell division cycle 6	CDC6	NM_001254	0.04
cell division cycle 20B	CDC20B	NM_152623	0.04
cyclin B2	CCNB2	NM_004701	0.05
DNA damage inducible transcript 3	DDIT3	NM_004083	0.06
baculoviral IAP repeat containing 5	BIRC5	NM_001168	0.07
cell division cycle 25C	CDC25C	NM_001790	0.08
cyclin A2	CCNA2	NM_001237	0.08
cell division cycle 2	CDC2	NM_001786	0.2
BRCA1, DNA repair associated	BRCA1	NM_007294	0.2
aurora kinase B	AURKB	NM_004217	0.2
RAD51 recombinase	RAD51	NM_002875	0.3
mutL homolog 1	MLH1	NM_000249	0.3
checkpoint kinase 1	CHEK1	NM_001274	0.4
Cell death			
baculoviral IAP repeat containing 5	BIRC5	NM_001168	0.01
Interferon beta 1	IFNB1	NM_002176	0.07
BCL2, apoptosis regulator	BCL2	NM_000633	0.5
Growth factor activity			
neuregulin 1	NRG1	NM_004495	0.08
fibroblast growth factor 23	FGF23	NM_020638	0.1
platelet derived growth factor subunit A	PDGFA	NM_002607	0.1
vascular endothelial growth factor A	VEGFA	NM_003376	0.3
brain derived neurotrophic factor	BDNF	NM_001709	0.3
fibroblast growth factor	FGF2	NM_002006	0.4
vascular endothelial growth factor B	VEGFB	NM_003377	0.5

Cell adhesion			
collagen type XXI alpha 1 chain	COL21A1	NM_030820	0.05
C-C motif chemokine receptor 1	CCR1	NM_001295	0.2
tenascin C	TNC	NM_002160	0.2
collagen type XVIII alpha 1 chain	COL18A1	NM_030582	0.2
collagen type XII alpha 1 chain	COL12A1	NM_004370	0.3
claudin 19	CLDN19	NM_148960	0.3
claudin 8	CLDN8	NM_012132	0.3
periostin	POSTN	NM_006475	0.4
claudin 7	CLDN7	NM_001307	0.5
Cell surface receptor linked signaling pathway			
platelet derived growth factor subunit A	PDGFA	NM_002607	0.1
C-C motif chemokine receptor 1	CCR1	NM_001295	0.2
fibroblast growth factor receptor 4	FGFR4	NM_002011	0.4
epiregulin	EREG	NM_001432	0.5
Intracellular signaling pathway			
DNA damage inducible transcript 3	DDIT3	NM_004083	0.06
C-C motif chemokine receptor 1	CCR1	NM_001295	0.2
neuregulin 1	NRG1	NM_004495	0.2
high mobility group box 2	HMGB2	NM_002129	0.2
BRCA1, DNA repair associated	BRCA1	NM_007294	0.2
proliferating cell nuclear antigen	PCNA	NM_002592	0.3
checkpoint kinase 1	CHEK1	NM_001274	0.4
fibroblast growth factor 2	FGF2	NM_002006	0.4
Cytokine activity			
TNF superfamily member 15	TNFSF15	NM_005118	0.06
pleiotrophin	PTN	NM_002825	0.4
growth differentiation factor 15	GDF15	NM_004864	0.4
CKLF like MARVEL transmembrane domain containing 4	CMTM4	NM_178818	0.4
Small inducible cytokine subfamily E, member 1	SCYE1	NM_004757	0.5
TNF superfamily member 13	TNFSF13	NM_003808	0.5
Signal transduction			
hyaluronan mediated motility receptor	HMMR	NM_012484	0.01

cell division cycle 6	CDC6	NM_001254	0.04
BRCA2, DNA repair associated	BRCA2	NM_000059	0.06
cyclin A2	CCNA2	NM_001237	0.08
BUB1 mitotic checkpoint serine/threonine kinase	BUB1	NM_004336	0.08
calcium/calmodulin dependent protein kinase I	CAMK1	NM_003656	0.1
period circadian clock 2	PER2	NM_003894	0.1
C-C motif chemokine receptor 1	CCR1	NM_001295	0.2
high mobility group box 2	HMGB2	NM_002129	0.2
fibroblast growth factor binding protein 1	FGFBP1	NM_005130	0.2
proliferating cell nuclear antigen	PCNA	NM_002592	0.3
vascular endothelial growth factor A	VEGFA	NM_003376	0.3
cryptochrome circadian clock 1	CRY1	NM_004075	0.3
checkpoint kinase 1	CHEK1	NM_001274	0.4
high mobility group box 1	HMGB1	NM_002128	0.5
period circadian clock 3	PER3	NM_016831	0.5
Proteolysis			
caspase 9	CASP9	NM_001229	0.5
Apoptosis			
baculoviral IAP repeat containing 5	BIRC5	NM_001168	0.01
BUB1 mitotic checkpoint serine/threonine kinase B	BUB1B	NM_001211	0.04
interferon beta 1	IFNB1	NM_002176	0.07
caspase 9	CASP9	NM_001229	0.5
cytochrome c, somatic	CYCS	NM_018947	0.5
Response to stress			
BRCA2, DNA repair associated	BRCA2	NM_000059	0.06
cyclin A2	CCNA2	NM_001237	0.08
C-C motif chemokine receptor 1	CCR1	NM_001295	0.2
high mobility group box 2	HMGB2	NM_002129	0.2
BRCA1, DNA repair associated	BRCA1	NM_007294	0.2
mutL homolog 1	MLH1	NM_000249	0.3
proliferating cell nuclear antigen	PCNA	NM_002592	0.3
vascular endothelial growth factor A	VEGFA	NM_003376	0.3
ATM serine/threonine kinase	ATM	NM_000051	0.4
sterol regulatory element binding transcription factor 1	SREBF1	NM_004176	0.4

CCAAT/enhancer binding protein gamma	CEBPG	NM_001806	0.4
checkpoint kinase 1	CHEK1	NM_001274	0.4
RAD51 recombinase	RAD51	NM_002875	0.4
mitogen-activated protein kinase kinase kinase kinase 2	MAP4K2	NM_004579	0.4
high mobility group box 1	HMGB1	NM_002128	0.5
epiregulin	EREG	NM_001432	0.5
BCL2, apoptosis regulator	BCL2	NM_000633	0.5
ATR serine/threonine kinase	ATR	NM_001184	0.5
RAD50 double strand break repair protein	RAD50	NM_005732	0.5
Inflammatory response			
C-C motif chemokine receptor 1	CCR1	NM_001295	0.2
Immune response			
TNF superfamily member 15	TNFSF15	NM_005118	0.06
C-C motif chemokine receptor 1	CCR1	NM_001295	0.2
BCL2, apoptosis regulator	BCL2	NM_000633	0.5
Multicellular organismal development			
neuropilin 1	NRP1	NM_003873	0.05
neuregulin 1	NRG1	NM_004495	0.08
calcium/calmodulin dependent protein kinase I	CAMK1	NM_003656	0.1
frizzled class receptor 1	FZD1	NM_003505	0.1
brain derived neurotrophic factor	BDNF	NM_001709	0.3
SMAD family member 1	SMAD1	NM_005900	0.4
homeobox A7	HOXA7	NM_006896	0.4
homeobox A6	HOXA6	NM_024014	0.4
hes family bHLH transcription factor 7	HES7	NM_032580	0.4
fibroblast growth factor 2	FGF2	NM_002006	0.4
msh homeobox 2	MSX2	NM_002449	0.4
periostin	POSTN	NM_006475	0.4
ATR serine/threonine kinase	ATR	NM_001184	0.5

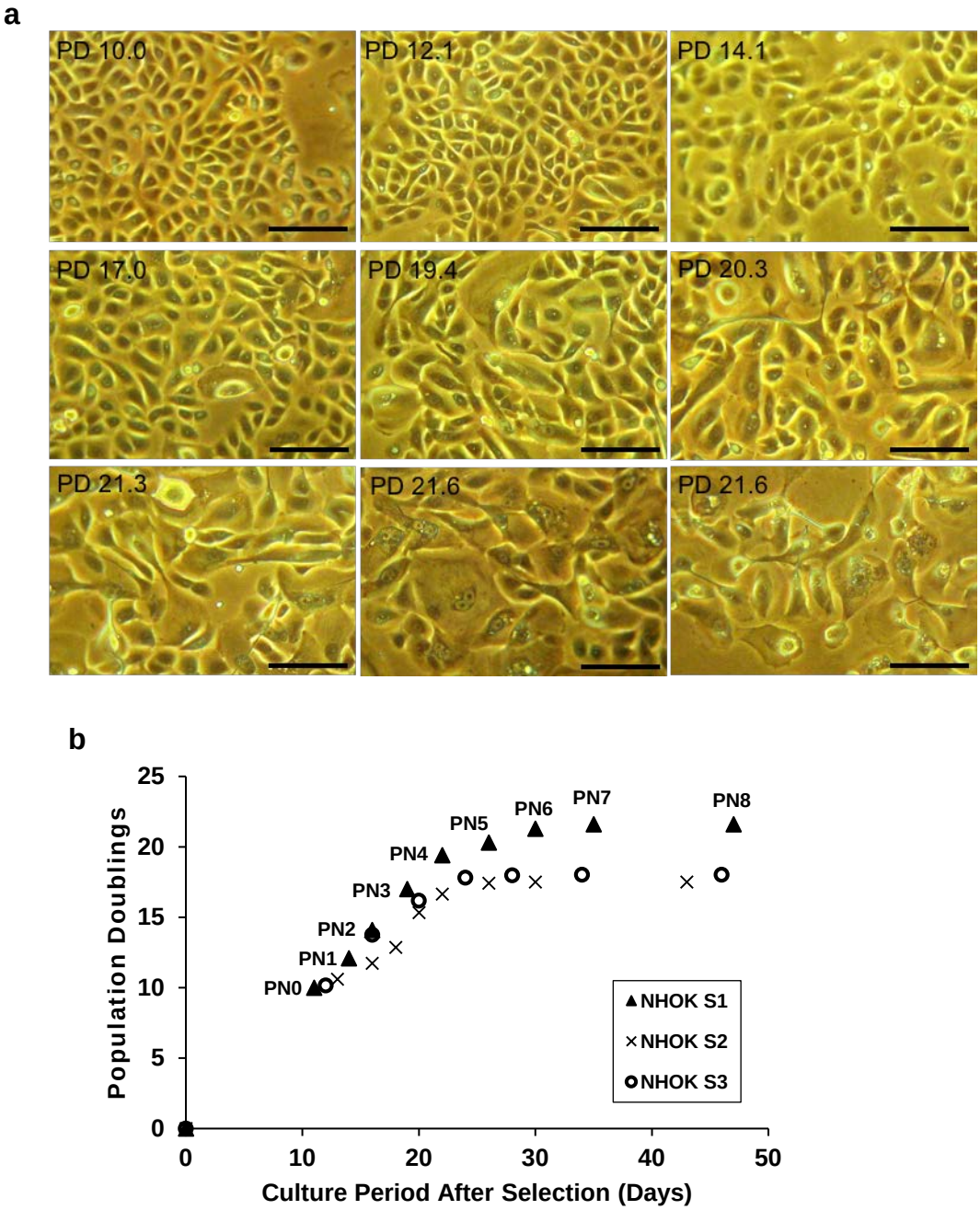

Figure 3. Cellular replication of serial subculture primary normal human oral keratinocytes (NHOKs) *in vitro*. (**a**) Microscopic features of NHOKs with increasing PDs. Scale bar is 100 μm. (**b**) Primary NHOK cultures from three different donors were serially passaged until the cells stopped dividing.

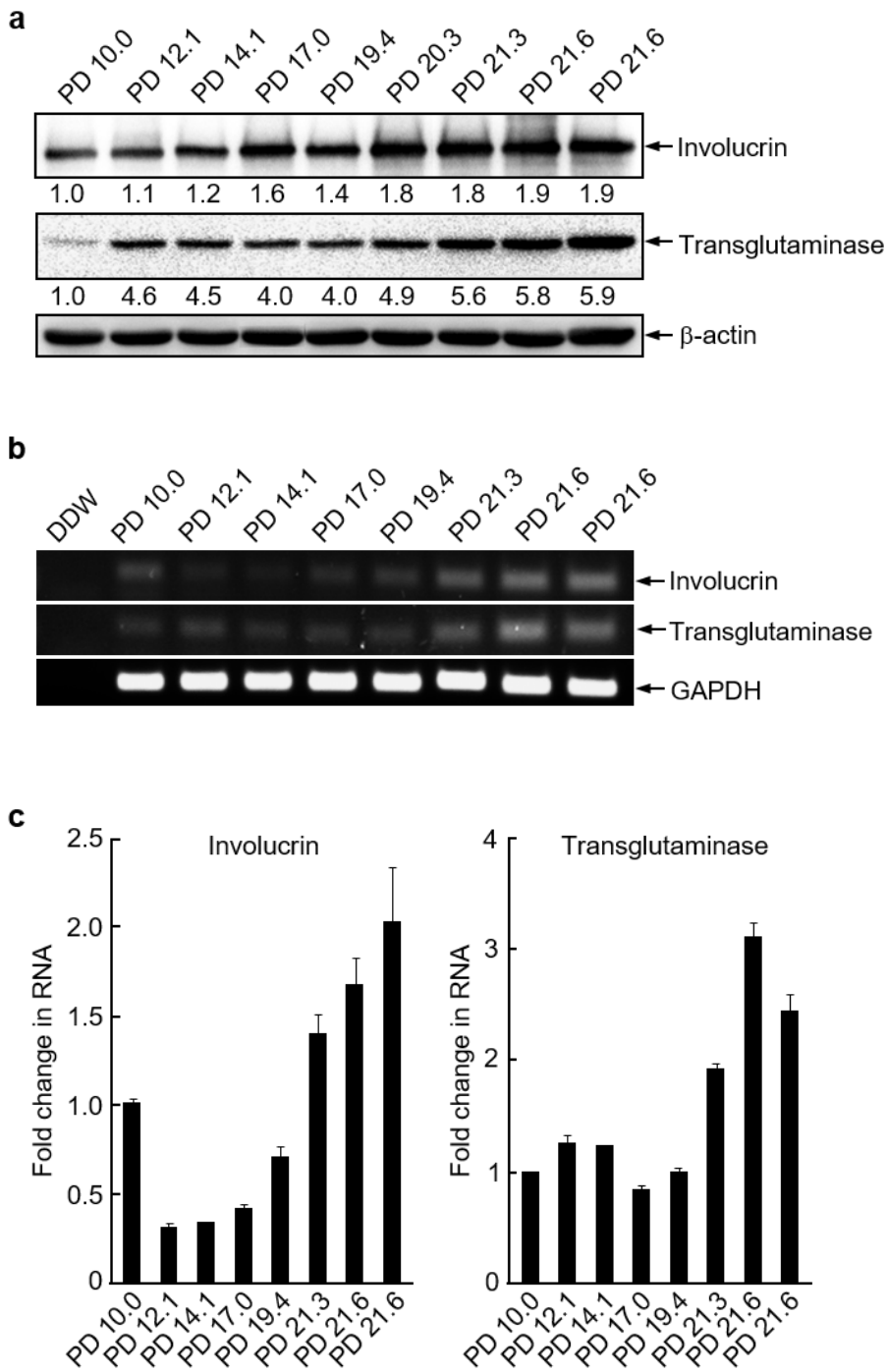
a
PD 10.0
PD 12.1
PD 14.1
PD 17.0
PD 19.4
PD 20.3
PD 21.3
PD 21.6
PD 21.6
Involucrin
1.0 1.1 1.2 1.6 1.4 1.8 1.8 1.9 1.9
Transglutaminase
1.0 4.6 4.5 4.0 4.0 4.9 5.6 5.8 5.9
β-actin
b
DDW
PD 10.0
PD 12.1
PD 14.1
PD 17.0
PD 19.4
PD 21.3
PD 21.6
PD 21.6
Involucrin
Transglutaminase
GAPDH
c
Involucrin
Fold change in RNA
2.5
2.0
1.5
1.0
0.5
0
PD 10.0
PD 12.1
PD 14.1
PD 17.0
PD 19.4
PD 21.3
PD 21.6
PD 21.6
Transglutaminase
Fold change in RNA
4
3
2
1
0
PD 10.0
PD 12.1
PD 14.1
PD 17.0
PD 19.4
PD 21.3
PD 21.6
PD 21.6

Figure 4. Differentiation associated gene expression in NHOKs with different PDs. (**a**) Levels of involucrin and transglutaminase proteins in NHOKs. β-actin served as a control for the differences in the staring amount of protein. (**b** and **c**) Expression of differentiation markers, including involucrin and transglutaminase, was measured by RT-PCR (**b**) and real-time PCR (**c**) analysis. RT-PCR for GAPDH was used as a loading control, and a reaction without input nucleic acid was run in the first lane as a negative control. Data are expressed as the mean ± SD (n = 3).

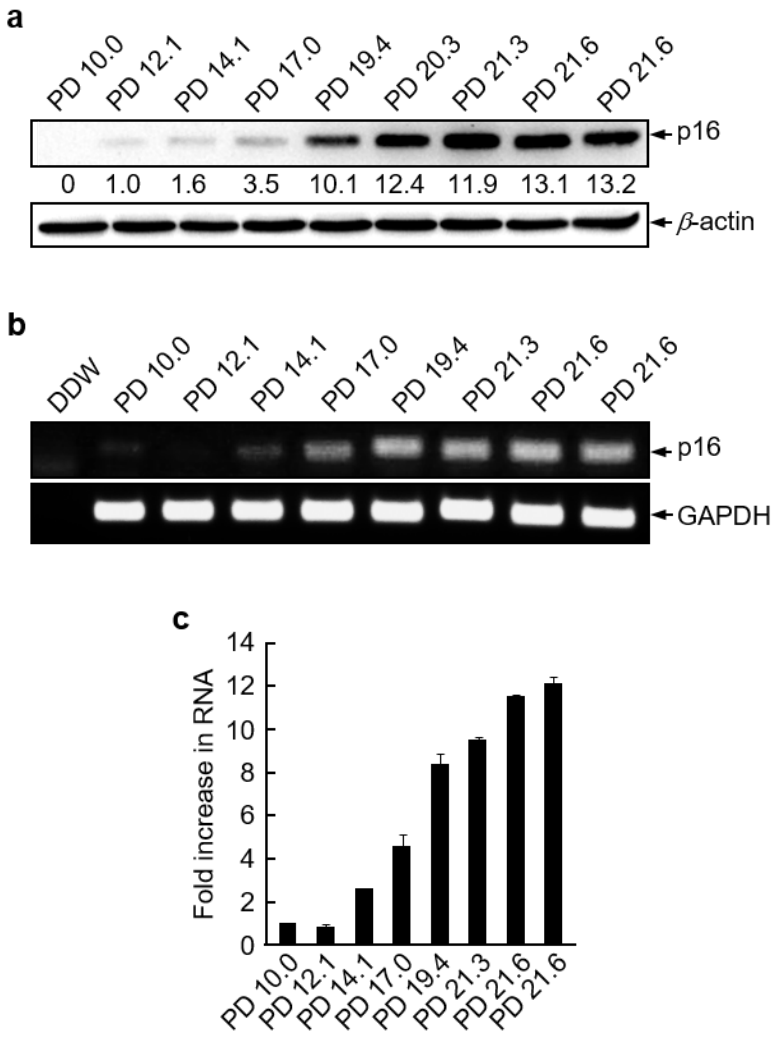
a
PD 10.0
PD 12.1
PD 14.1
PD 17.0
PD 19.4
PD 20.3
PD 21.3
PD 21.6
PD 21.6
p16
0 1.0 1.6 3.5 10.1 12.4 11.9 13.1 13.2
β-actin
b
DDW
PD 10.0
PD 12.1
PD 14.1
PD 17.0
PD 19.4
PD 21.3
PD 21.6
PD 21.6
p16
GAPDH
c
Fold increase in RNA
0
2
4
6
8
10
12
14
PD 10.0
PD 12.1
PD 14.1
PD 17.0
PD 19.4
PD 21.3
PD 21.6
PD 21.6
d
PD 12.1
PD 18.1
e
PD 12.1
PD 18.1

Figure 5. Senescence associated gene expression in NHOKs with different PDs. (**a**) Western blot analysis of $p16^{INK4A}$ in NHOKs. (**b** and **c**) Expression of $p16^{INK4A}$ was measured by RT-PCR (**b**) and real-time PCR (**c**) analysis. Data are expressed as the mean ± SD (n = 3). (**d**) Microscopic features of the exponentially growing (PD 12.1) and terminally differentiated and replicative senescent (PD 18.1) NHOKs. (**e**) Phase-contrast micrographs of senescence-associated β-galactosidase staining (SA-β-gal staining) of the exponentially growing (PD 14.1) and terminally differentiated and senescent (PD 21.6) NHOKs. The culture conditions were the same as described in the legend to Fig. 3a. Scale bar is 100 μm.

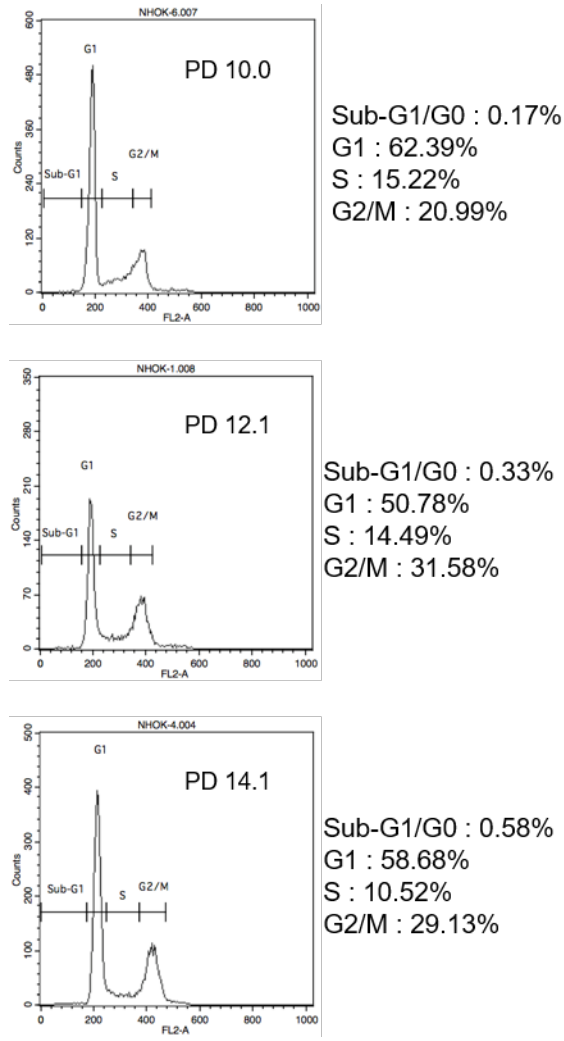

Figure 6. Cell cycle profile analysis. NHOKs (PD 10.0, 12.1 and 14.1) were submitted to flow cytometry analyses.

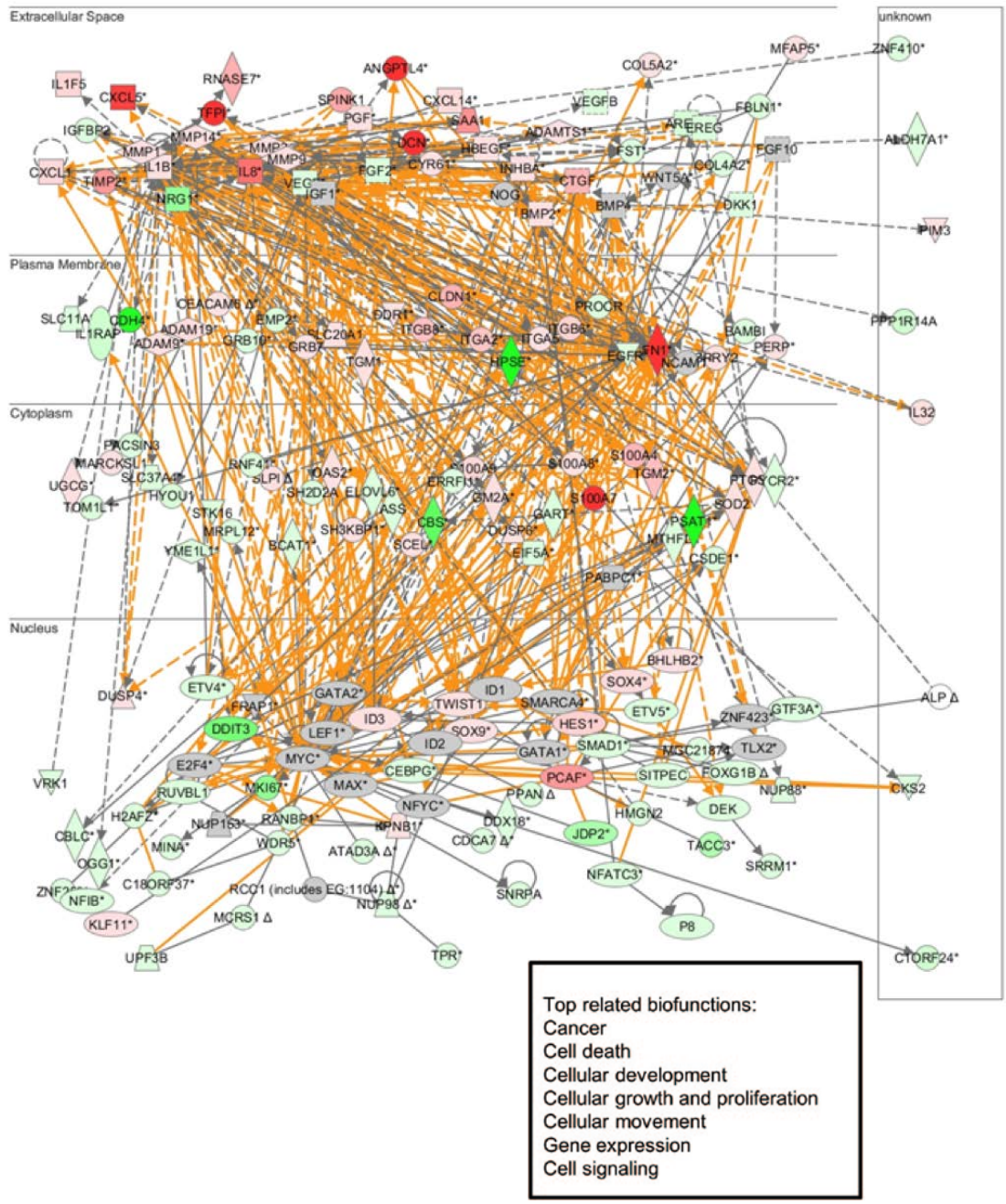

Figure 7. An integrated network with both upregulated and downregulated genes in the exponentially growing (PD 14.1) and terminally differentiated and senescent (PD 21.6) NHOKs. Dataset was analyzed by the Ingenuity Pathways Analysis software. The top scoring network of annotated genes significantly regulates by serial subculture at PD 21.6 relative to PD 14.1. Red indicates upregulation and green indicates downregulation.

a

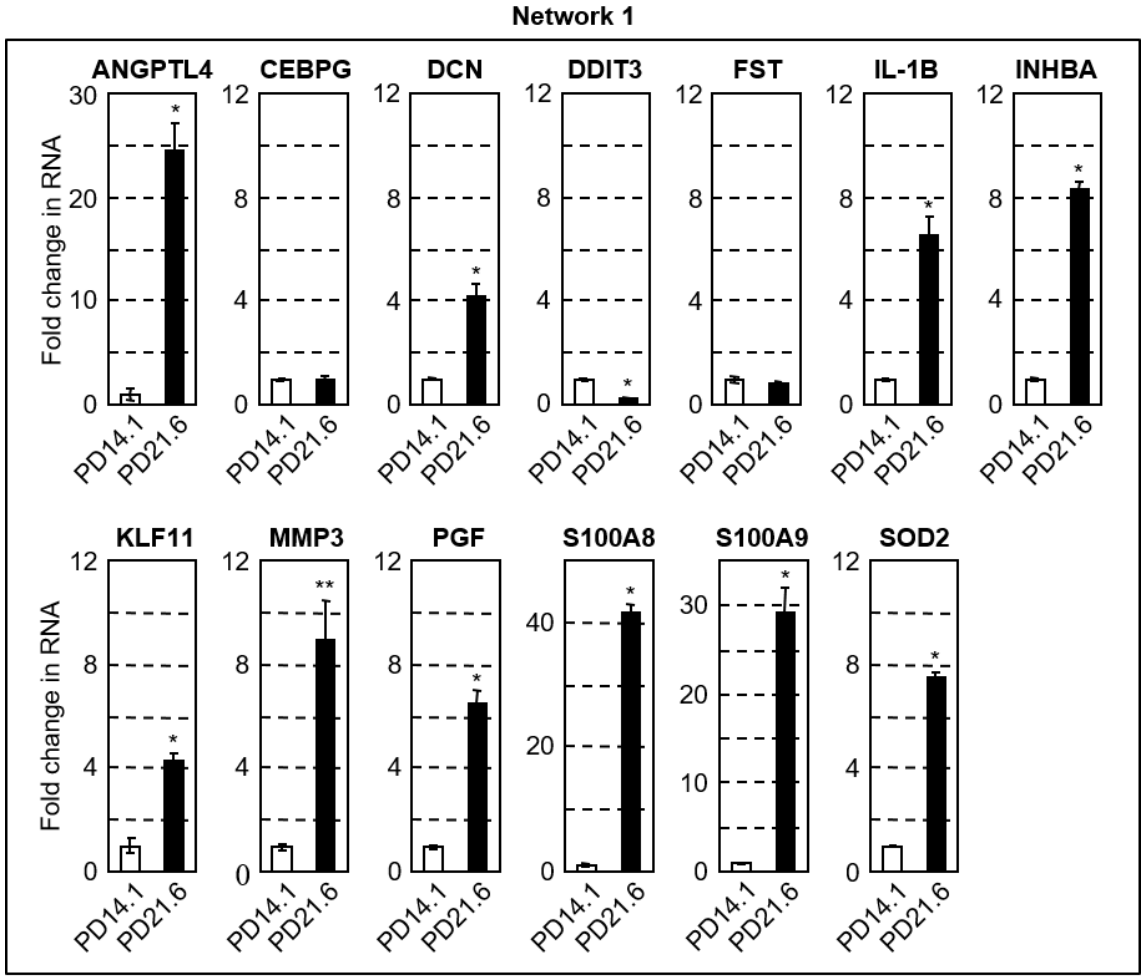

Figure 8a. Measurement of mRNA levels of some genes in network 1 by real-time RT-PCR during subculture-induced cell differentiation and senescence in NHOKs. Data are expressed as mean ± SD (n = 3). *$p < 0.01$, **$p < 0.05$.

b

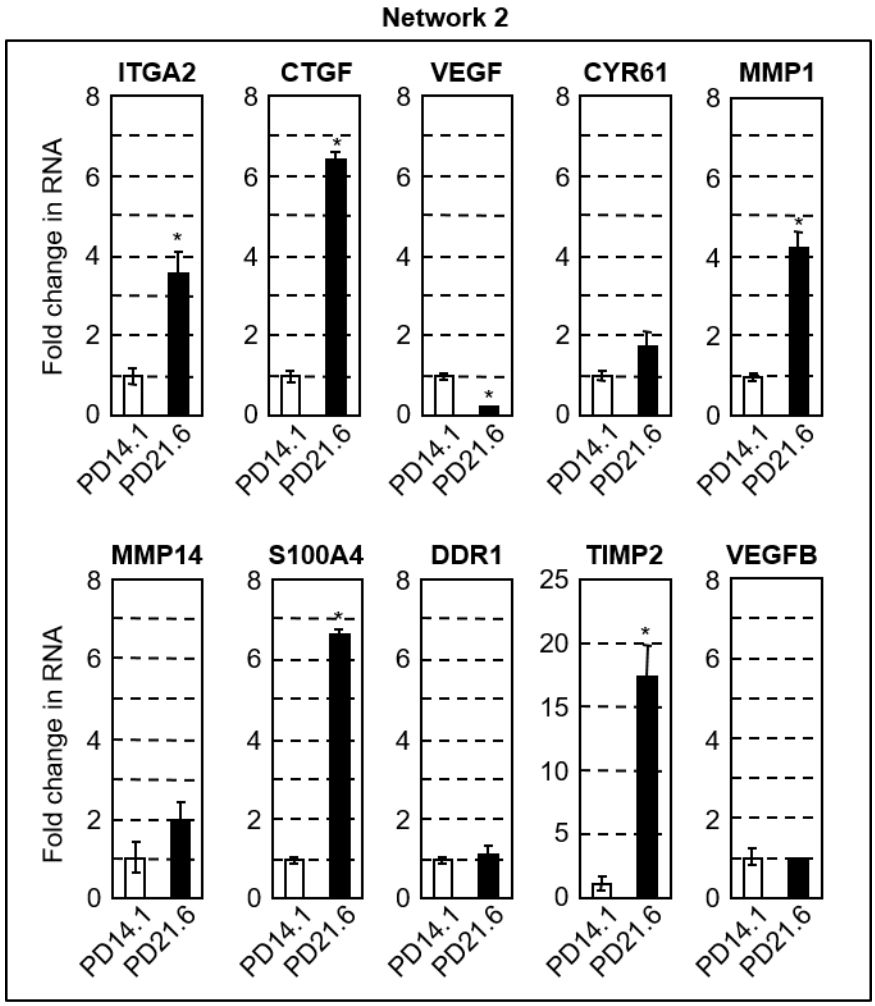

Figure 8b. Measurement of mRNA levels of some genes in network 2 by real-time RT-PCR during subculture-induced cell differentiation and senescence in NHOKs. Data are expressed as mean ± SD (*n* = 3). **p < 0.01, **p < 0.05*.

c

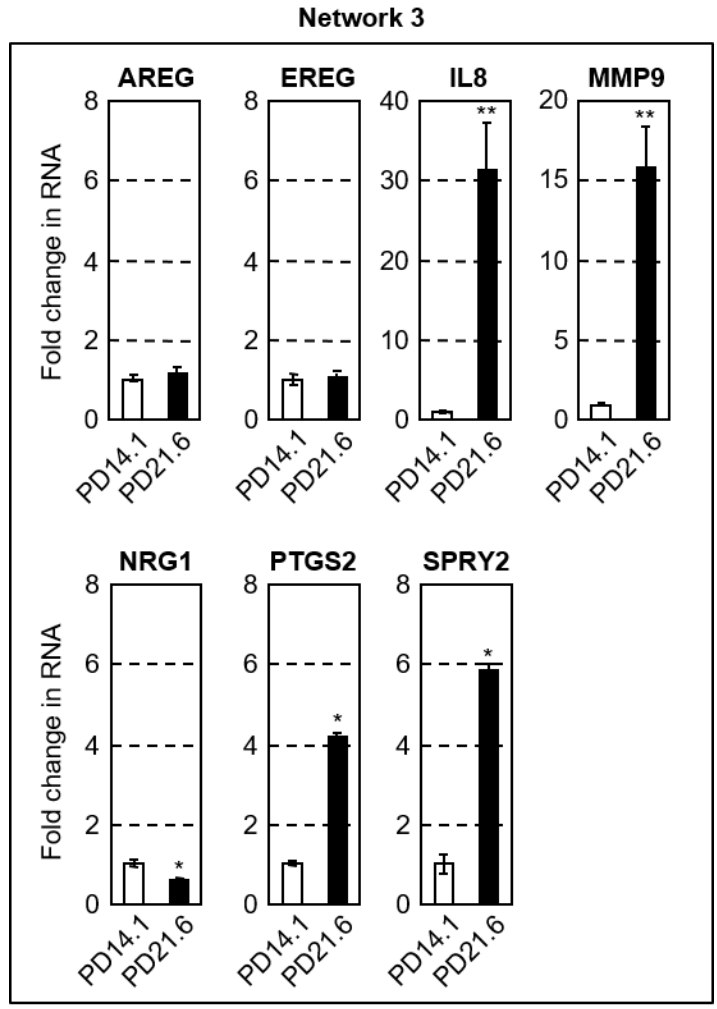

Figure 8c. Measurement of mRNA levels of some genes in network 3 by real-time RT-PCR during subculture-induced cell differentiation and senescence in NHOKs. Data are expressed as mean ± SD (*n* = 3). *$p < 0.01$, **$p < 0.05$.

d

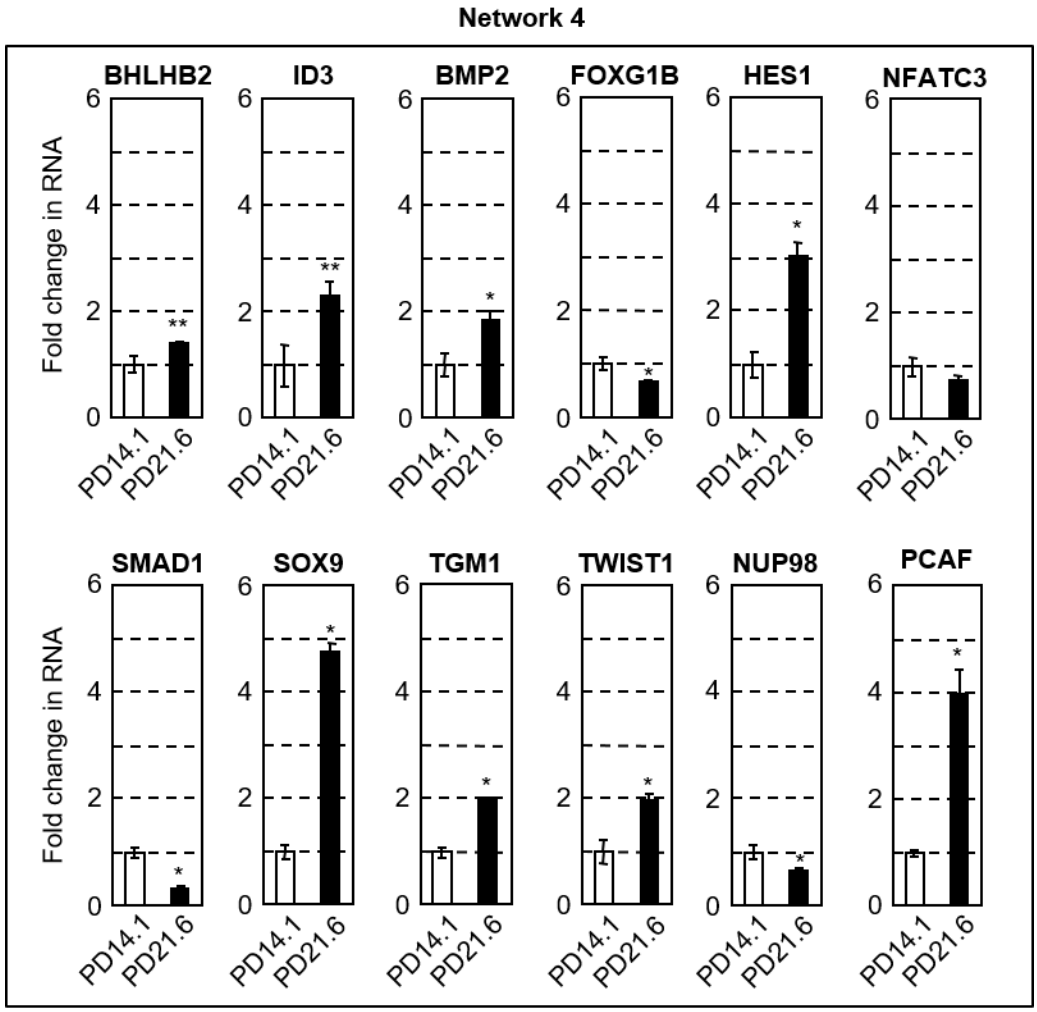

Figure 8d. Measurement of mRNA levels of some genes in network 4 by real-time RT-PCR during subculture-induced cell differentiation and senescence in NHOKs. Data are expressed as mean ± SD (n = 3). *$p < 0.01$, **$p < 0.05$.

e

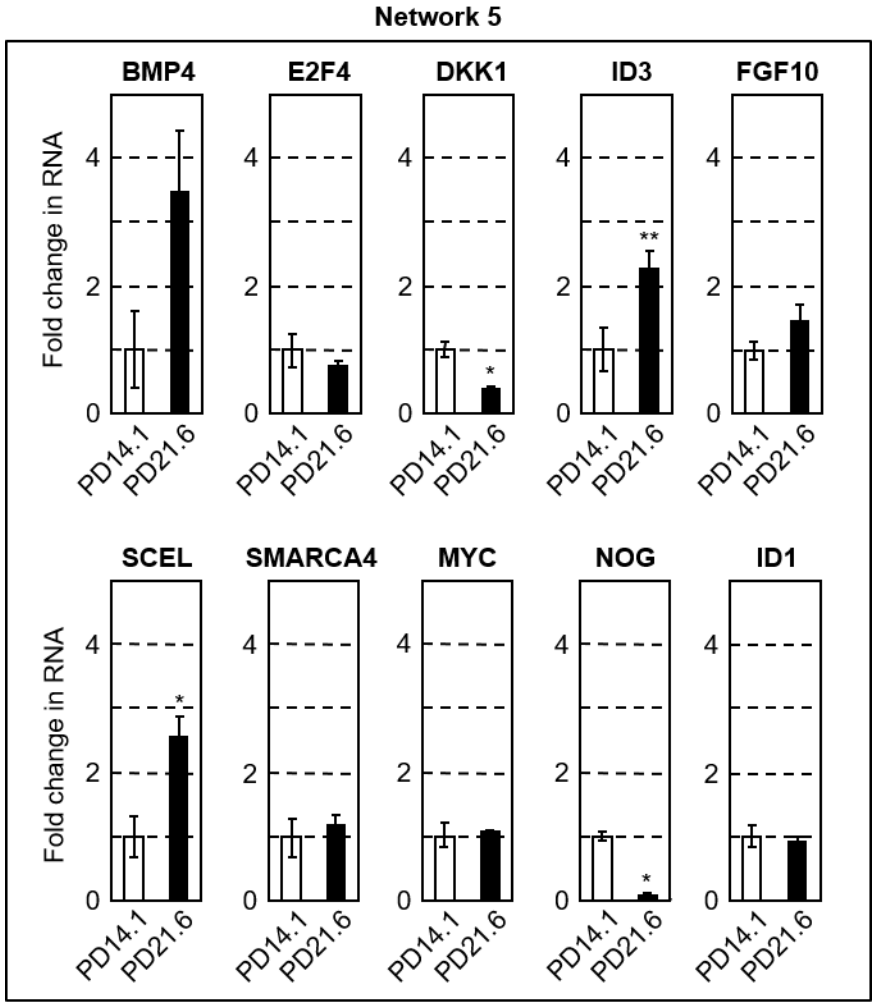

Figure 8e. Measurement of mRNA levels of some genes in network 5 by real-time RT-PCR during subculture-induced cell differentiation and senescence in NHOKs. Data are expressed as mean ± SD (n = 3). *$p < 0.01$, **$p < 0.05$.

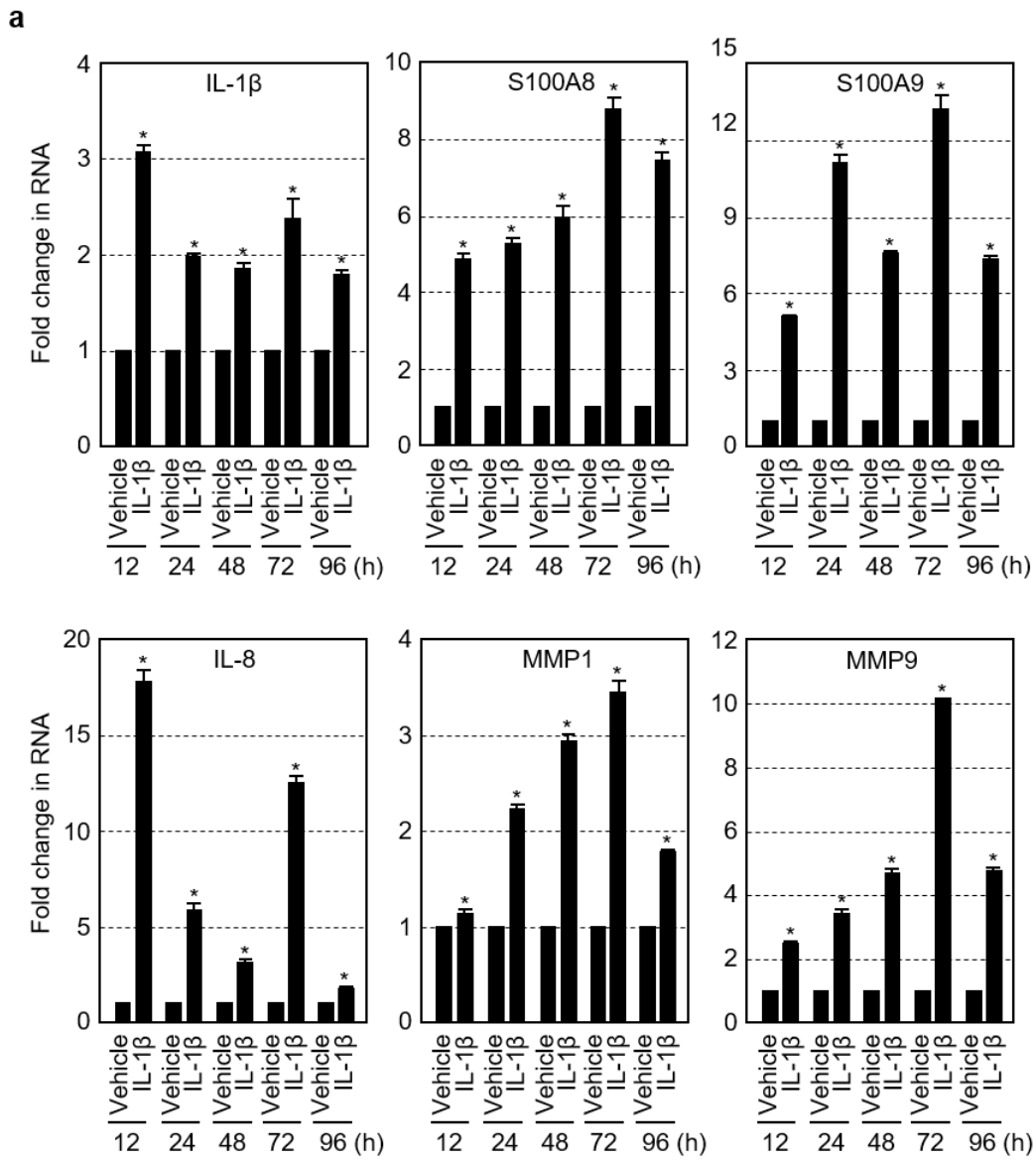

Figure 9a. Effects of IL-1β on the expression of inflammatory molecules in primary normal human oral keratinocytes (NHOKs). (**a**) Levels of IL-1β, S100A8, S100A9, IL-8, MMP1, MMP9, and VEGF mRNAs in NHOKs treated with IL-1β. Exponentially growing NHOKs were incubated with 10 ng/ml of recombinant human IL-1β for 12, 24, 48, 72, and 96 h. Total RNA was isolated and subjected to quantitative real-time PCR. Data are expressed as fold change over vehicle-treated cells at each time point. Data are expressed as mean ± SD (n = 3). *$p < 0.01$.

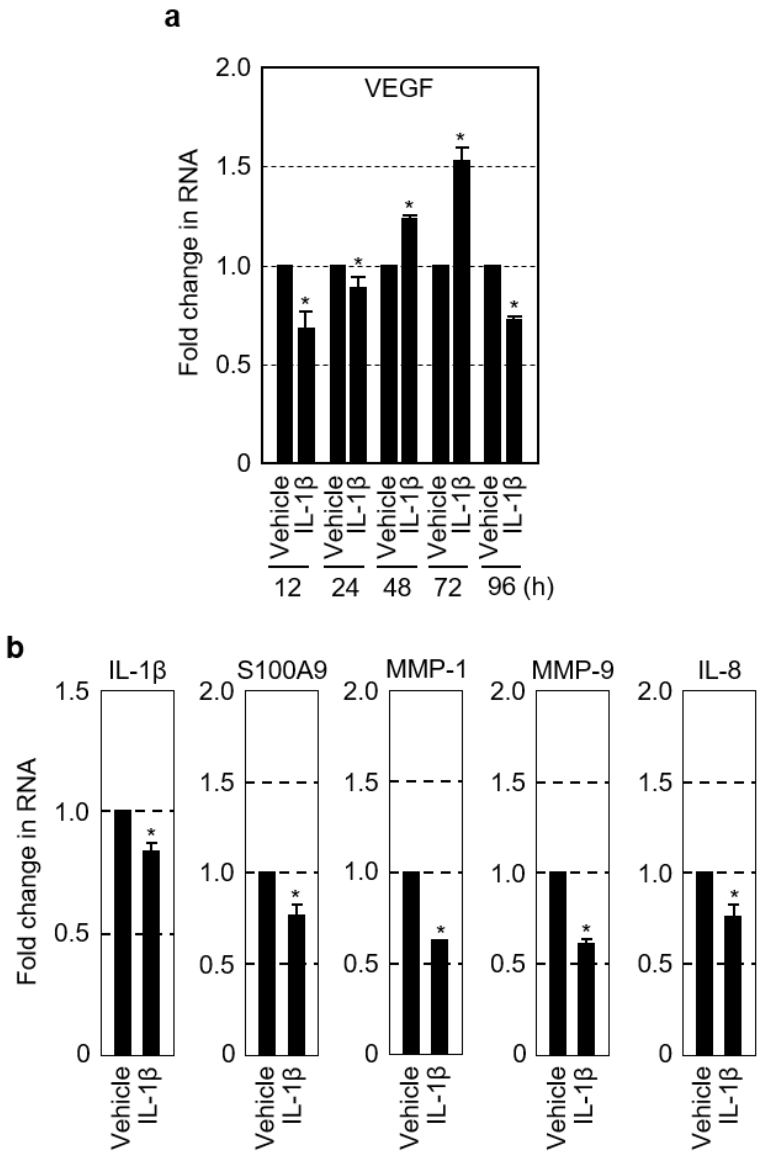

Figure 9b. Effects of IL-1β/IL-1F2 on the expression of inflammatory molecules in primary human oral keratinocytes. (**b**) Levels of IL-1β, S100A9, MMP1, MMP9, and IL-8 mRNAs in terminally differentiating and senescent cells treated with IL-1β/IL-1F2 neutralizing antibody (10 ng/ml) for 14 days. Data are expressed as mean ± SD (n = 3). *$p < 0.01$.

a

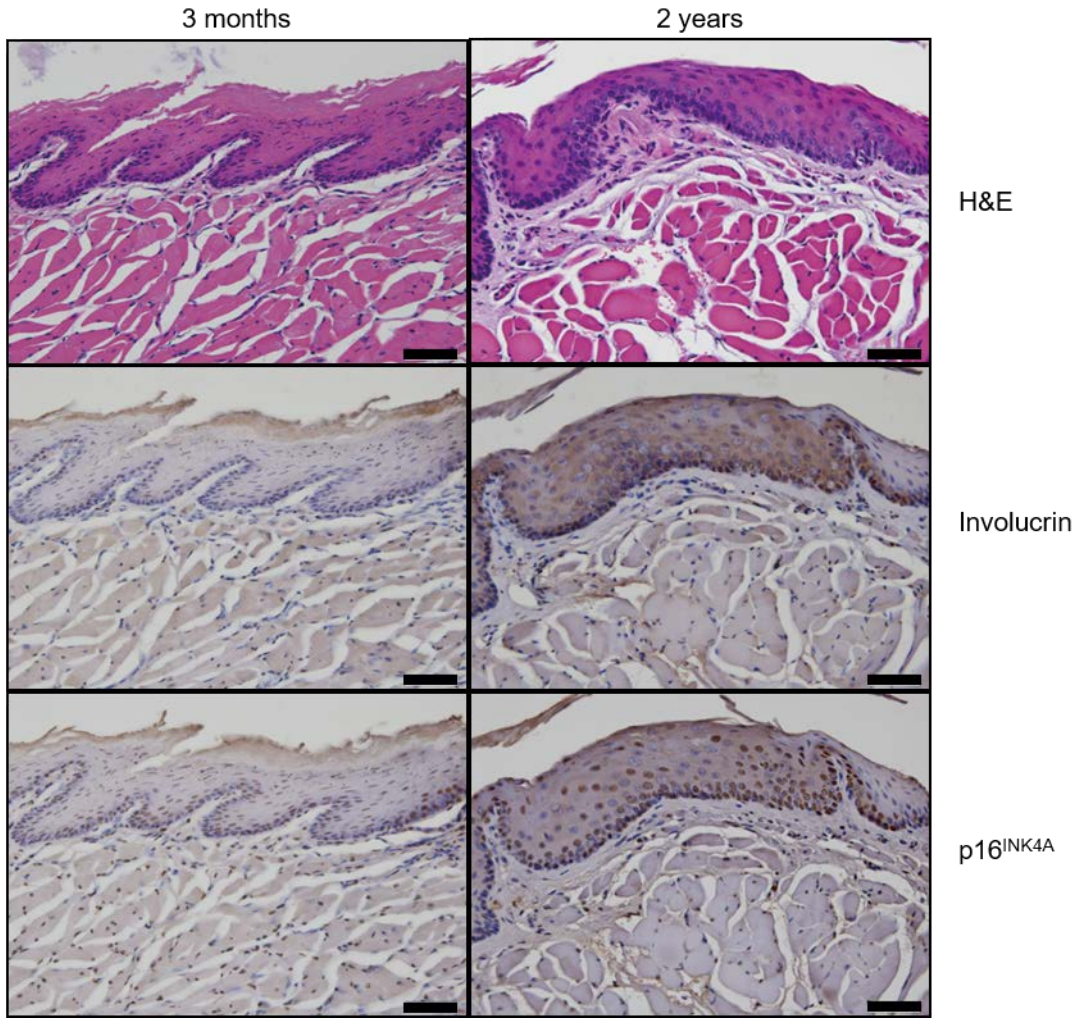

Figure 10a. H&E staining and immunohistochemical analysis of involucrin, p16INK4A in gingiva of young (3 months) and old (2 years) mice. 4 μm thick sections of formalin-fixed and paraffin-embedded mice gingival tissues were deparaffinized, and immunoreactivity was detected using the DAKO ENVISION Kit. Scale bar is 20 μm.

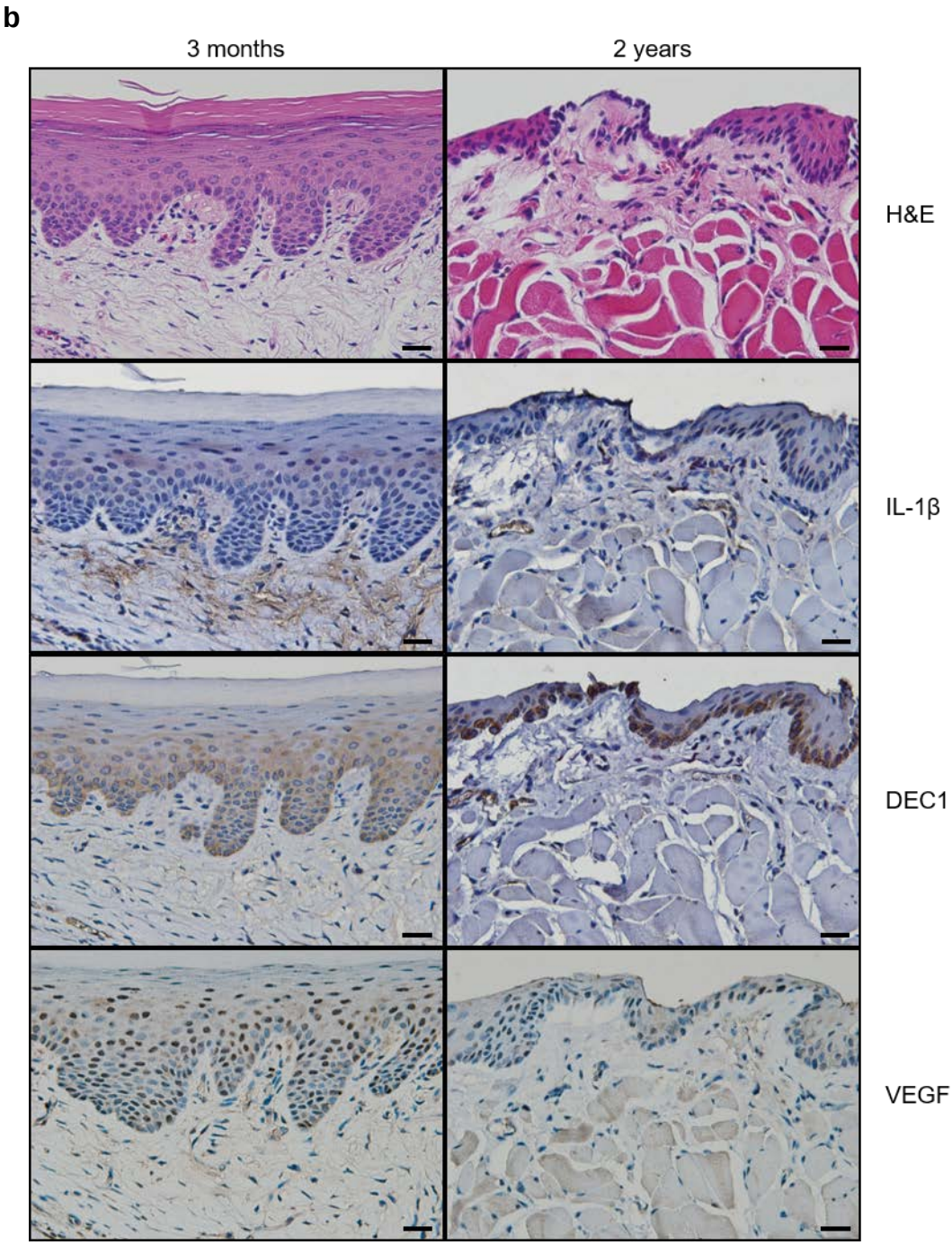

Figure 10b. H&E staining and immunohistochemical analysis of IL-1β, DEC1, and VEGF in gingiva of young (3 months) and old (2 years) mice. 4 μm thick sections of formalin-fixed and paraffin-embedded mice gingival tissues were deparaffinized, and immunoreactivity was detected using the DAKO ENVISION Kit. Scale bar is 20 μm.

국문 초록

사람 구강각화세포의 최종분화 및 복제노화 과정에서 유전자 발현 프로파일링

장 다 현

종양 및 발달 생물학 전공

서울대학교 치의학대학원

(지도교수: 민 병 무, D.D.S., M.S., Ph.D.)

체세포(somatic cells)는 제한된 복제능력을 갖고 있으며, 일정 횟수의 세포분열 후 텔로미어 단축(telomere shortening)에 의해 DNA 손상이 촉발됨으로서 더 이상 DNA 복제를 하지 못하고 비가역적으로 세포분열 정지상태에 도달하는데 이를 복제노화라고 한다. 또한 복제노화가 일어난 세포는 비록 대사활성은 유지하고 있지만 형태학적 변화와 유전자 발현에 큰 차이를 보인다. 분화와 노화관련 유전자들에 관한 연구는 오래 전부터 수행되어 왔지만 사람 정상 상피세포의

최종분화 및 복제노화 과정에서 관련유전자를 포괄적으로 분석하고, 그의 네트워크와 주요기능 분석에 관한 연구는 아직 완전히 밝혀지지 않았다. 그러므로 본 연구는 사람 정상 구강각화세포의 최종분화 및 복제노화 과정에서 이와 관련된 유전자 발현변화를 포괄적으로 분석하고, 이들 유전자들의 네트워크와 기능의 일단을 연구하였다. 사람 구강각화세포를 일차배양한 다음 연속적으로 계대배양을 시행하여 최종분화 및 복제노화가 일어난 세포들을 채득하였으며, 이들 세포에서 최종분화 및 복제노화가 유도되었음을 단백질 및 RNA 수준에서 확인하였다. 빨리 증식하는 구강각화세포와 최종분화 및 복제노화가 일어난 구강각화세포에서 tRNA를 분리한 다음 Affymetrix사의 Human Genome U133 Plus 2.0 Array를 이용하여 마이크로어레이를 시행하였다. 마이크로어레이에 의한 유전자 발현 결과는 real-time RT-PCR 방법으로 확인하였다. 또한 생물정보학 분석 소프트웨어인 Ingenuity Pathway Analysis (IPA)를 이용하여 최종분화 및 복제노화과정에서 얻은 유전자 발현 변화로부터 유전자 네트워크와 주요기능을 분석하였다. 또한 기능분석을 토대로 사람 구강각화세포에서 염증반응에 관련된 유전자의 기능을 연구하기 위하여 빨리 증식하는 사람 구강각화세포에 IL-1β를 12~96시간 처리하였으며, 최종분화 및 복제노화가 일어난 세포에 IL-1β 중화항체를 14일간 처리한 후 분석하였다. 나아가 이를 생체조직에서 확인하기 위하여, 생후 3개월 된 쥐와 생후 2년 된 쥐의 치은조직에서 최종분화 및 복제노화관련 유전자 발현을 면역세포화학염색법으로 확인하였다. 일차배양한 사람 정상 구강각화세포를 연속적으로 계대배양 시 최종분화 및 복제노화가 유도됨을 단백질 및 RNA 수준에서 확인하였다. 최종분화

및 복제노화가 일어난 사람 구강각화세포에서 1,247종의 유전자는 발현이 증가되었고 1,219종의 유전자는 발현이 감소되었다. 발현이 변화된 유전자들은 주로 수송, 세포증식, 세포주기, 면역반응, 세포사멸, 전사 및 염증반응에 관여하는 유전자들이었다. 또한 사람 구강각화세포의 최종분화 및 복제노화가 일어남에 따라 IL-1β, S100A8, S100A9, MMP1, MMP9, IL-8, BHLHB2, HES1 및 TWIST1 유전자의 발현이 현저하게 높아졌다. 염증유발관련 유전자(IL-1β 및 IL-8) 발현이 높은 것을 확인하기 위하여 IL-1β 및 IL-1β 중화항체를 사람 정상 구강각화세포에 처리한 결과, IL-1β 처리한 세포에서는 IL-1β, S100A8, S100A9, MMP1, MMP9 및 IL-8의 발현이 증가하였으나 IL-1β 중화항체를 처리한 세포에서는 발현이 감소하였다. 또한 생체의 노화된 조직에서 최종분화 및 복제노화 관련유전자의 발현변화를 연구한 결과, 생후 3개월 된 쥐와 비교할 때 생후 2년 된 쥐의 치은조직에서 involucrin과 $p16^{INK4A}$의 발현이 증가되었으며, DEC1(Bhlhb2)과 IL-1β 발현이 증가됨을 확인하였다. 이상의 연구결과, 사람 구강각화세포의 최종분화 및 복제노화 과정에서 유전자 발현변화를 포괄적으로 분석하였으며, 나아가 분자 네트워크 및 생물학적 주요 기능의 일단을 밝혀 사람 정상 상피세포의 분화 및 노화과정을 이해하는데 큰 도움을 줄 것으로 생각된다.

주요어: 사람 구강각화세포, 세포분화, 복제노화, 유전자 네트워크

학 번: 2008-22047